Rivista Italiana di Paleontologia e Stratigrafia	volume 114	no. 3	pp. 431-452	November 2008

THE TRIASSIC/JURASSIC BOUNDARY IN A PERITIDAL CARBONATE PLATFORM OF THE PELAGONIAN DOMAIN: THE MOUNT MESSAPION SECTION (CHALKIDA, GREECE)

ROBERTA ROMANO [1*], DANIELE MASETTI [1], NICOLAOS CARRAS [2], FILIPPO BARATTOLO [3] & GUIDO ROGHI [4]

Received: March 12, 2008; accepted: August 31, 2008

Key words: Triassic/Jurassic boundary, biostratigraphy, facies analysis, peritidal cyclicity, Pelagonian Domain, Greece.

Abstract. In the Mount Messapion area (Chalkida, Greece) a continuous and expanded section of Triassic/Jurassic (T/J) limestone is exposed. This section consists of a 710 m thick pile of shallowing-upward peritidal cycles; the persistence of the facies and the lack of paleoenvironmental changes across the T/J boundary allowed studying the distribution of shallow water microfossils. The T/J boundary is placed in the upper part of the section defined by correspondence with (i) the last occurrence of *Triasina hantkeni*, (ii) the abrupt disappearance of megalodontid faunas and (iii) the presence of Early Jurassic microfossil assemblages. This paleontological reorganization happens suddenly, it is not controlled by any facies change, and surprisingly, it seems to produce no evident modification in the vertical stacking pattern of the cycles. A detailed facies analysis, performed along a 290 m thick stratigraphic interval (60 m above the T/J boundary and 230 m below), allowed the recognition of peritidal cycles: five different elementary cyclothemes are described and their distribution along the section is given. This integrated stratigraphic study attempts to highlight the relationship between the changes of carbonate producers and sea level fluctuations across the T/J boundary.

Riassunto. A Monte Messapion (Chalkida, Grecia) affiora con buona continuità di affioramento una potente successione stratigrafica di età Triassico Superiore-Giurassico Inferiore. La sezione consiste in circa 710 m di cicli peritidali *shallowing upward*; la persistenza delle facies e la mancanza di cambiamenti paleoambientali nell'intervallo stratigrafico contenente il limite Triassico-Giurassico (T/J) ha permesso un accurato studio delle distribuzioni dei microfossili di ambiente di mare poco profondo. Il limite T/J nella porzione superiore della sezione è stato posto in corrispondenza della concomitante (a) scomparsa di *Triasina hantkeni*, (b) definitiva scomparsa delle faune a megalodontidi, (c) presenza delle prime associazioni di microfossili del Giurassico Inferiore. Il cambiamento nella composizione paleontologica avviene repentinamente e non sembra causare alcuna modificazione nell'organizzazione verticale dei cicli. Una accurata analisi delle facies applicata ad un intervallo di 290 metri (60 metri sotto il limite T/J e 230 al di sopra), ha permesso la descrizione di cinque diversi ciclotemi elementari: questi sono stati descritti attraverso una dettagliata analisi delle diverse litofacies che li compongono. La distribuzione dei diversi cicli elementari lungo la sezione è fornita assieme ad un'interpretazione ciclostratigrafica della loro organizzazione verticale. Lo studio stratigrafico integrato (biostratigrafia ed analisi di facies) oggetto di questo lavoro, rappresenta il primo tentativo di mettere in evidenza, in ambiente di piattaforma carbonatica interna, le possibili relazioni intercorrenti tra le variazioni del livello del mare e i cambiamenti che hanno interessato i produttori di carbonato al limite T/J.

Introduction

Processes and causes of biotic change at the Triassic/Jurassic (T/J) transition and its outcome on the depositional environments still remain controversial. Recent studies (Hesselbo et al. 2007), focused on the slope and basinal deposits and obtained by multidisciplinary investigations, have helped the recognition of the latest Triassic-earliest Jurassic events: the position of the T/J boundary is currently constrained by radiolarian, conodont and ammonoid biostratigraphy, chemostratigraphy and magnetostratigraphy. In shallow water successions, the location of the T/J boundary is often debata-

1 DISGAM, Dipartimento di Scienze Geologiche, Ambientali e Marine, Università di Trieste, via Weiss, 2- 34127, Trieste, Italy. *corresponding author. E-mail: robroman@unina.it; masetti@units.it
2 IGME, Messoghion 70, GR-11527 Athens, Greece. E-mail: nicarras@igme.gr
3 Università degli Studi di Napoli Federico II, Dipartimento di Scienze della Terra, L.go San Marcellino, 10 - 80138, Napoli, Italy. E-mail: lippolo@unina.it
4 Istituto di Geoscienze e Georisorse - CNR, via Matteotti, 30 - 35121, Padova, Italy. E-mail: guido.roghi@igg.cnr.it

ble, whether for the scarcity of sections studied in detail, or for the very poor fossil content characterizing the lower Hettangian platform deposits, often affected by a pervasive dolomitization.

In addition, the biostratigraphic schemes utilized in shallow marine environment, based on benthic foraminifers and green algae, are characterized by several discrepancies affecting the biozonal limits. (Hottinger 1967; Septfontaine 1984, 1986; De Castro 1991; Chiocchini et al. 1994; Bassoullet 1997a,b; Barattolo & Romano 2005; Wilmsen & Neuweiler 2008). Actually, the range of the index taxa lacks a good calibration and correlation with other biostratigraphically more meaningful fossil groups. The recent paper of BouDagher & Bosence (2007) is a meritorious attempt to utilize new species of *Siphovalvulina* as taxa-index for the Hettangian – lower Sinemurian biozonation. Unfortunately, also this biostratigraphic scheme lacks of any kind of chronostratigraphic constrains.

The difficulties in the discrimination between upper Triassic and lower Jurassic beds leave unresolved the characterization of the biotic and environmental change in shallow water platforms. The scarcity of data in shallow water environment at the T/J boundary may seem surprising if compared to the contemporary huge spreading of carbonate platforms systems in the Mediterranean area. These carbonate systems developed along the southern margin of the Neotethys are always characterized by the occurrence of thick peritidal cyclic successions. The Upper Triassic platform carbonates have been named Dachstein Limestone, while the dolomitic ones are well known as the Dachstein Dolomite or Hauptdolomit, although the lithostratigraphic terminology of this unit may differ regionally. The following units represent different examples of Upper Triassic shallow-water carbonate successions belonging to several Tethyan domains: the Zu Limestone (Western Southern Alps, Jadoul et al. 1992; Galli et al. 2005, 2007), Dolomia Principale and Calcare di Dachstein, (Eastern Southern Alps, Bosellini 1967; Bosellini & Hardy 1988; Cozzi et al. 2005; Berra et al. 2007, cum bibl.); Sciacca and Inici formations (Sicily, Petti 2007 and ref. therein), Csovár Formation (Hungary, Haas 2004; Pálfy et al. 2007 and ref. therein), Fatra Formation (Western Carpathian, Michalík et al. 2007 and ref. therein); Pantocrator Limestone (Greece, Partsch 1887; Schäfer & Senowbari-Daryan 1982; Haas & Skourtsis-Coroneou 1995; Pomoni-Papaiaoannou et al. 1986). Haas (2004) gives an exhaustive bibliographic outline of the studies on the Upper Triassic platform deposits, since the 19th century.

According to Ciarapica synthesis (2007), the first environmental changes inside these Tethyan platform systems occur from late Norian. These changes are linked to the development of the oceanic branches related to the Pangea breakup and well identified in the paleogeographic restorations for the early Mesozoic (see for example: Ciarapica & Passeri 1998, 2002, 2005; Stampfli & Borel 2002; Finetti 2005). As a consequence of the fragmentation of the Pangea at the T/J boundary and of other events occurring at the Sinemurian/Pliensbachian boundary (Masetti et al. 2006), the Early Jurassic paleogeography of the southern margin of the Tethys exhibits a composite scenario characterized by many platform-basin depositional systems, each one with a different sedimentary evolution.

The researches carried out in the last years on the timing and mode of end -Triassic biotic crisis (Hesselbo et al. 2007; Barattolo & Romano 2005) represent the starting point of this work. Several sections dealing with carbonate platform crossing the Triassic/Jurassic boundary located in the Southern Alps (Trento and Friuli Platforms), Central and Southern Apennines and Sicily have been examined by the authors of this paper (Barattolo & Romano 2005), but the best example of a continuous and undolomitized section has been found in Greece, in the Mt. Messapion (Chalkida). This section, studied through a multidisciplinary approach, provides an excellent case-history for a better understanding of the environmental and biological events which occurred across the T/J boundary and their mutual relationships.

Geological setting

The Mt. Messapion section is situated at the NE part of the Thivai (Thebes) map sheet, 10 Km west of Chalkis city (today named and written Halkida or Chalkida) (Fig. 1), between the hairpin bends N38°27'52,92" E23°28'20,52" and N38°27'40,2" E23°29'46,2" of the road that leads to the summit (Fig. 2). The same outcrop also exposed the NW part of the adjacent Halkida map sheet, on the eastern slope of Mt. Messapion.

In the Thivai sheet the Messapion section exposes to an "Upper Triassic - Lower Malm" sequence which consists of "*dolomites and dolomitic limestones of upper Triassic age on the lower parts of the south-southeast slopes of the Messapion Mountain. They continue with white-grey microcrystalline limestones with* Triasina hantkeni *Majzon, of Rhaetian-Hettangian age. These limestones underlie conformably the unit with* Orbitopsella *and occur on the south slopes of the Messapion and Ypaton mountains. On the west and northwest piedmont of the mountain Ypaton there are white-grey limestones of lower early to upper Jurassic age with* Labyrinthina mirabilis, Saccocoma *sp.,* Haplophragmoides *sp.,* Kilianina *and algae*" (Tataris et al. 1970). The presence of the Upper Jurassic (with *Cladocoropsis*) in the area is

Fig. 1 - Location map of Mt. Messapion area in east-central Greece.

also documented by Renz & Reichel (1948). In the Thivai sheet the sequence is ascribed to the so called Eastern Greece zone (Subpelagonian).

Recently (Parginos et al. 2007, Halkida sheet) the same formation, ascribed to the "Pelagonian zone unit of non-metamorphic formations", is described as follows: "*Middle Triassic – Middle Lias: Limestones, dolomitic limestones and dolomites (Tm-Ji.k): gray to white-grey, medium- to thick-bedded, locally unbedded, usually microcrystalline, and strongly tectonized. At the Mt. Ktypas and Galatideza red limestone intercalations occur of small thickness. At the southern margins of Ktypas Mt. big* Megalodon *are observed (up to 25 cm diameter)".* The underlying formation (Fig. 3) is constituted of "*sandstones, microconglomerates, shales and spilites basalts (Ti.sh): slightly metamorphic series consisting of clastic sediments, lenticular limestone layers (Ti.k) and schistose spilites-basalts and keratophyric tuffs*". In the lenticular limestone layers, Early Triassic conodonts were found.

The Middle Triassic – Pliensbachian limestones are truncated upwards by the "*Eohellenic Tectonic Nappe", constituted of "ultrabasic rock masses (o) and volcano-sedimentary formations (b.sh) overthrust...during the end of Jurassic and the beginning of Cretaceous*".

Such a succession is typical of the Pelagonian Domain, which is represented by a wide Upper Triassic – Lower Jurassic carbonate platform that, in some places survived up to the Late Jurassic. This carbonate platform was destroyed during the late Jurassic before the deposition of a mélange, accompanying the pre-Late Cretaceous overthrust of the ophiolitic nappe and the transgressive Upper Cretaceous formations (Celet & Ferrière 1978; Celet et al. 1988).

The ophiolitic nappe, or better the "Eohellenic Tectonic Nappe", directed from NE to SW, and covering the East part of the Pelagonian, is constituted of formations representing an oceanic crust, as well as by formations of the ocean borders and immense masses of peridotites. All these elements were tectonically intercalated in the Pelagonian succession near the Jurassic end and beginning of the Cretaceous (Katsikatsos 1979), in correspondence of the Eohellenic Tectonic Phase (the "*révolution fini-jurassique*" of Dercourt

Fig. 2 - Southern view of Mt. Messapion. The section is placed along the second hairpin bend of the road. A and B mark respectively the start and the end of the studied section.

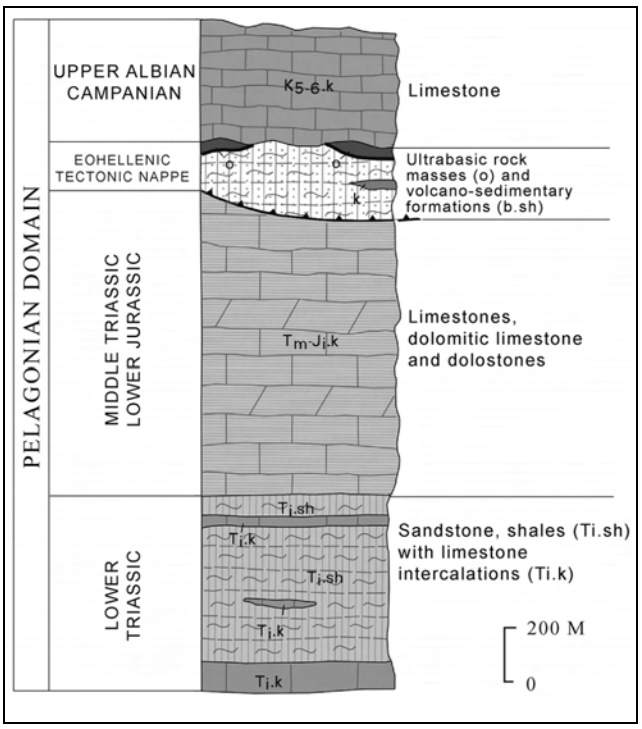

Fig. 3 - Synthetic stratigraphic column of the units of the Pelagonian domain.

1972), which is the key feature of the Internal Hellenides. The latest Jurassic – Early Cretaceous lateritization of the emerged ophiolitic nappe gave rise to Fe-Ni and/or bauxitic deposits, which developed on the ophiolites and/or in the karstic cavities of the nearby emerged limestones, of Late Triassic up to Late Jurassic age, depending on the depth of the erosion.

From the palaeogeographic point of view, most authors consider the Pelagonian as a part of the African/Apulian plate, along the south-western margin of the Vardar/Tethys Ocean (e.g. Dercourt et al. 1985, 1993; Ciarapica & Passeri 2002). Textural, geochemical and micropaleontological features indicate that the Pelagonian, comprising its NE edge, was an area of Southern Tethyan affinity, at least until Aptian times (Carras & Georgala 1998).

Mount Messapion section

To locate the T/J boundary in shallow water deposits of Eastern Greece has proved difficult. Large part of the Triassic - Lower Jurassic Pelagonian carbonate platform is metamorphosed or intensely tectonized. The Parnassus Carbonate Platform, representing a part of the Pelagonian domain at those times, is largely dolomitized in its eastern part, while, in the western part (Pendeoria area) the drowning of the platform was precocious, before this boundary. During the geological mapping of Chalkis sheet, a large outcrop comprising

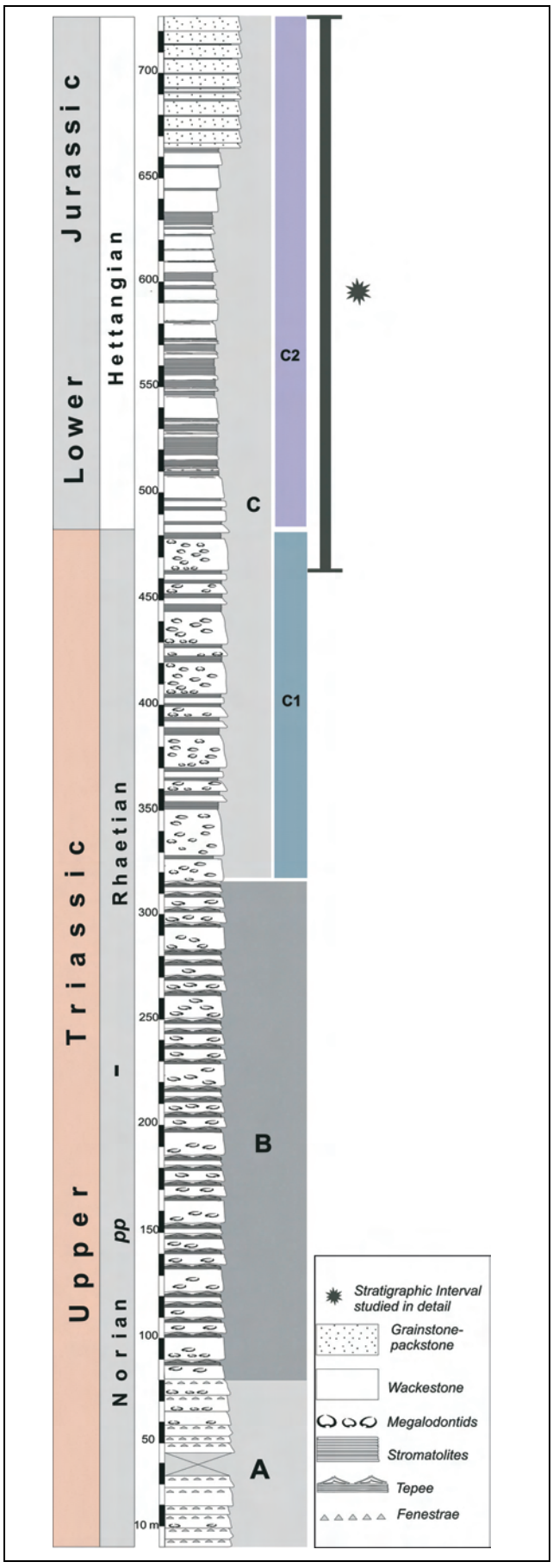

Fig. 4 - Generalized stratigraphy of the Mt. Messapion (see text for subdivision into Units A-C).

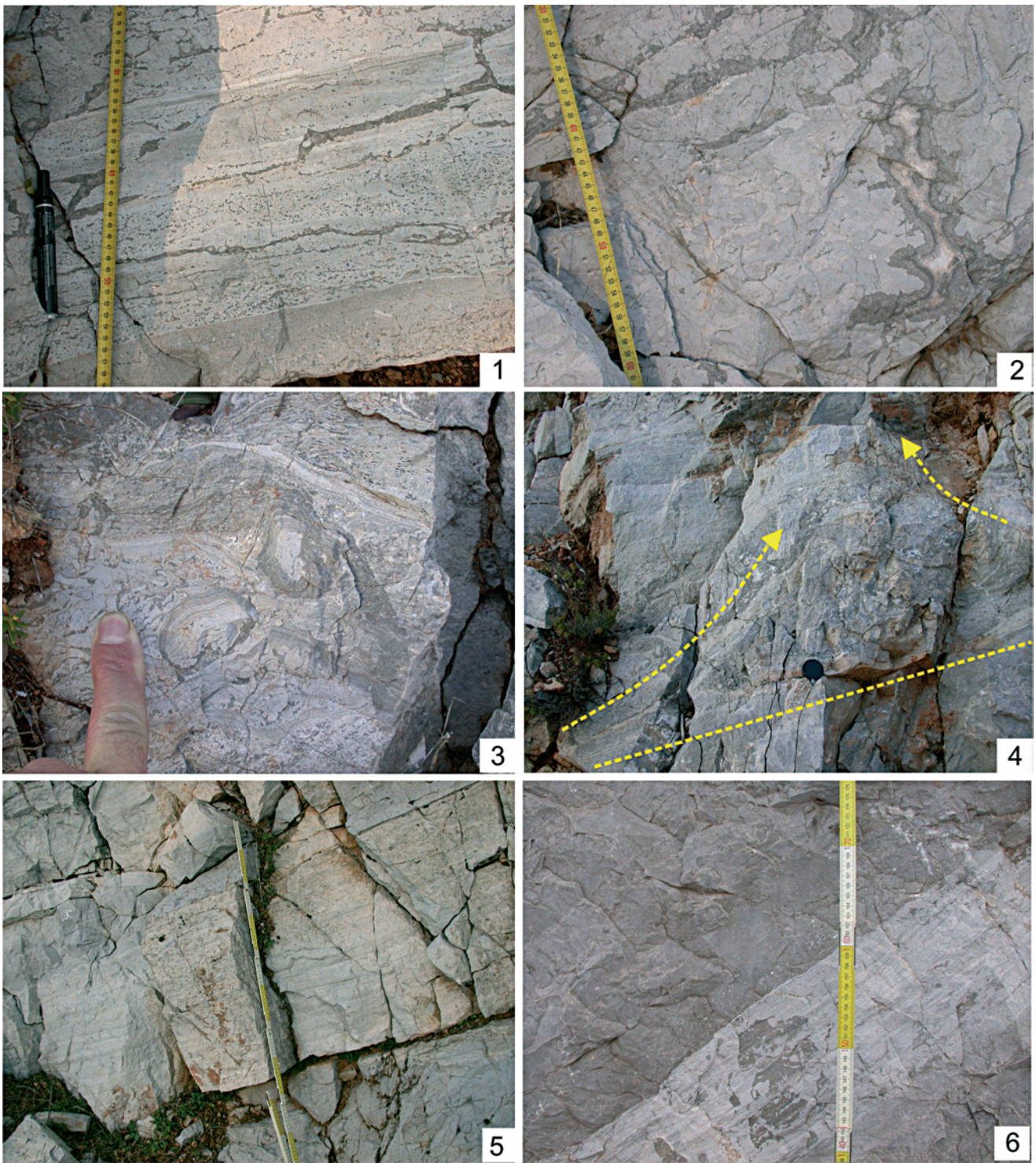

Fig. 5 - Mt. Messapion lithofacies. 1) Laminated loferites of Unit A; 2) dissolution surface penetrating in the underlying subtidal portion of the cycle. Unit A; 3) shelter voids associated to tepee structure, filled by a complex variety of internal sediment, pisoids, and cements showing geopetal fabrics. Unit B; 4) antiform tepee structures of the Unit B; 5, 6) microbialitic layers representing the inter and supratidal cap of the cycles in the subunits C1-C2.

a large part of the uppermost Triassic and of the overlying Lower Jurassic, without any important dislocations, was identified in the higher part of Mt. Messapion by dr. Anastasios Mavrides, who showed us the section, which is in the focus of this study.

This section outcrops along a military road leading up to the summit of Mt. Messapion which represents a smoothed monocline located in the north-eastern part of continental Greece, close to the western coast of the Chalkida channel (Figs 1-2). The Mt. Messapion section consists of a 710 metres thick pile of shallowing-upward, peritidal cycles. Their age is constrained by micro- and macrofossils such as foraminifers, green algae and bivalves (Barattolo & Romano

2005). The field work, focused on facies analysis and biostratigraphic study through detailed sampling of the succession, was performed during several field trips from 1999 to 2006. This lead us to establish the biostratigraphical constrains of the section and to identify three main superimposed units, defined chiefly on the basis of the features of its peritidal cycles (Fig. 4). From the base to the top, the Mt. Messapion section consists of the following units:

Unit A - 70 metres thick of meter-scale, shallowing-upward cycles in which the subtidal portion is made of bioclastic-intraclastic wackestone/packstones with rare megalodontids, passing gradually upward into supratidal, laminated loferites (Fig. 5.1). This part of the cycle is characterized by two main types of fenestral pores: irregular and laminoid fenestrae. These latter are sometimes characterized by a flat bottom and an irregular top, aligned according to the bedding planes; their origin is commonly related to the molds of cyanobacterial mats buried by sediment or to desiccation and propagation of sub-horizontal sheet cracks (Demicco & Hardie 1994). Laminoid fenestrae are common in the loferitic interval, but more frequently they alternate with other kinds of irregular fenestrae. In some instances the latter appear as just large intergranular pores or shelter voids beneath intraclasts (*pseudofenestrae* sensu Shinn 1983), unrelated to the shrinkage of the sediment during a subaerial exposure, thus suggesting a subtidal environment.

The loferitic interval is frequently characterized by very irregular dissolution cavities that penetrate up to 1 m into the underlying subtidal portion of the cycle (Fig. 5.2). These dissolution cavities often show a planar growth, frequently tabular and parallel to the stratification, sometimes with an irregular shape. They are filled with several generations of cements: the first phase of the cementation is represented by a fibrous isopachous cement of marine phreatic origin. This cement encrusts the wall of the cavity, whereas sparry calcite, formed during the late diagenetic burial phase occurs in the central part of the cavity. The irregular morphology of such cavities seems related to inter- or intragranular porosity. The dissolution processes involved the skeletal grains (bivalves, algae, etc.) and their internal cavities.

Megalodontid shells are frequently recognizable inside the meshwork system of cavity.

Unit B - 230 m of meter-scale peritidal cycles similar in thickness and organization to those described above in the Unit A. This unit differs from the underlying one by the presence of tepee structures inside the supratidal microbialitic cap overlying the subtidal, megalodontid-rich, bioturbated wackestone. The tepees are characterized by antiform deformation structures (Fig. 5.3) commonly associated with a suite of features related to subaerial exposures, including cross-cutting fractures, shelter voids filled by a complex variety of internal sediment, pisoids, and cements that display geopetal fabrics (Fig. 5.4). Sometimes tepee horizons are covered by onlapping microbialitic bindstones.

Unit C - 410 m of peritidal cycles without tepee structures. Each subtidal portion of the cycle is characterized by an inter -supratidal cap consisting of a well-developed microbialitic interval (Figs 5.5-6).

This 410 m thick unit can be divided into two sub-units, mainly on the basis of macroscopic features and the abrupt disappearance of megalodontids: C1 (the first 180 m) and C2 (the remaining 230 m). (Fig. 4)

The subunit C1 is made up of 180 metres of peritidal cycles characterized by a basal lag (only occasionally present), constituted by flat pebbles deriving from the stromatolitic layers at the top of the underlying cycle; a mudstone-wackestone subtidal unit, showing an intense bioturbation mainly produced by the megalodontid fauna.

This subtidal interval shows a gradual transition into the intertidal one, which is made of a slightly dolomitized stromatolitic layer alternating with a micritic horizon. The cycle is capped by an often dolomitized supratidal stromatolitic layer, with fenestrae, sheet crack and other features related to subaerial exposures. The thickness of the supratidal interval varies from some centimetres to few metres.

The subunit C2 is made up of 230 m of peritidal cycles similar to the subunit C1, but with the complete absence of megalodontids. The organization of these cycles shows a micritic and bioturbated subtidal interval with a characteristic basal lag, capped by the peritidal stromatolitic unit.

In the upper part of the interval C2 a gradual enrichment of oolitic bioclastic grainstone-packstone as well as an abundance of benthic foraminifers and green algae are observed. Gastropods and bivalves are present as well. In this upper portion several lithofacies can be recognized within the subtidal interval of the cycle. At the base of the bed, there is a lag composed by intraformational breccias with flat pebbles, gradually passing upward to a thin, mainly micritic lithofacies (mudstone and packstone), bearing small rounded intraclasts and peloids with dasycladaceae and benthic foraminifers. Upward, a gradual increase in size and abundance of grains leads to the superimposition of a grainy lithofacies on the former micritic portion. This grainy lithofacies is made up of packstone and grainstone with ooids, intraclasts, peloids and skeletal grains. The cycle is capped by a stromatolitic interval characteristic of inter- to supratidal environments.

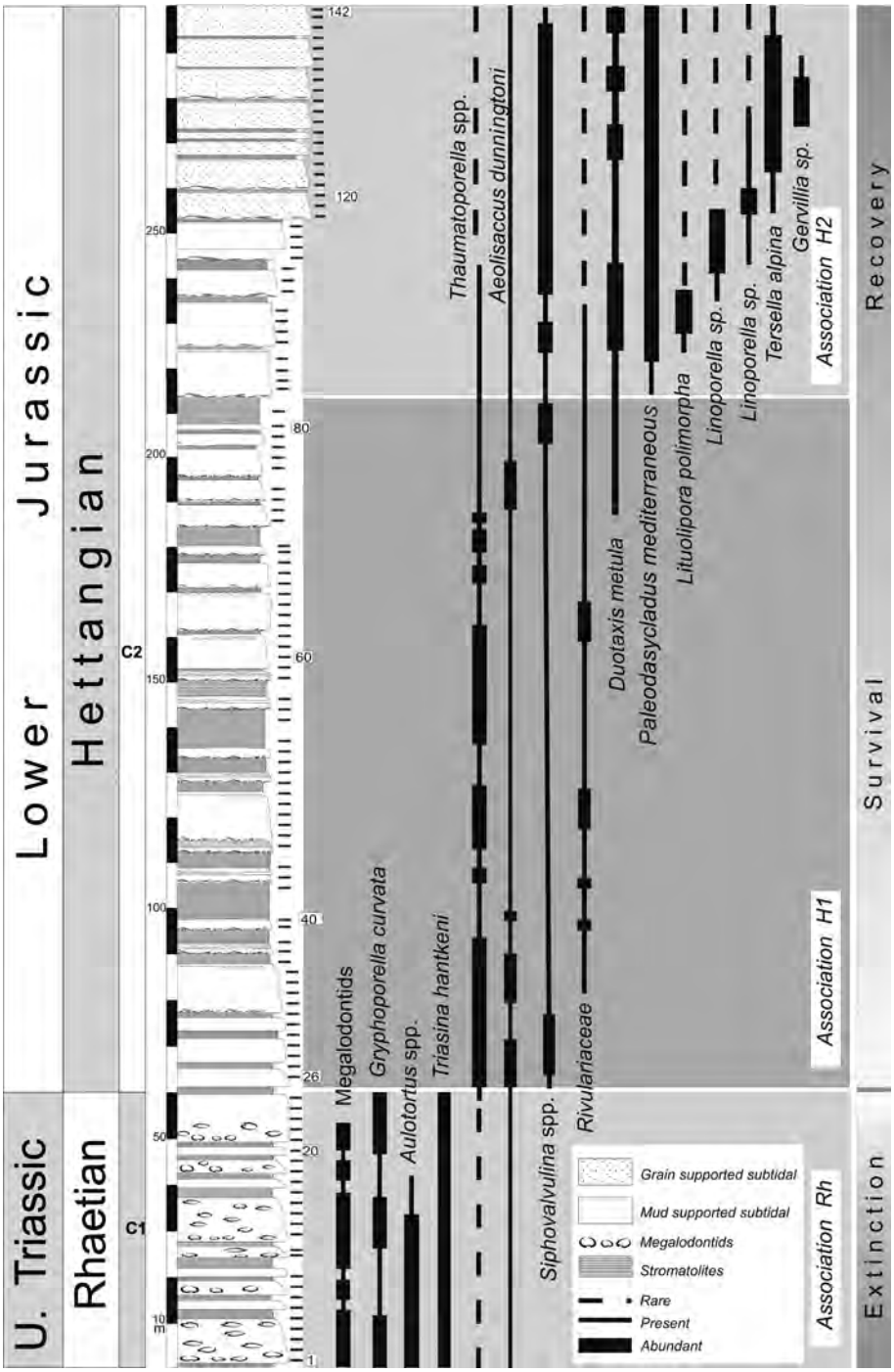

Fig. 6 - Range of the main taxa of the subunits C1 and C2 of the Mt. Messapion section.

Paleontology and biostratigraphy

Paleontological studies are focused on a 290 m thick interval containing the T/J transition. This interval corresponds to the upper portion (60 m) of subunit C1 plus the entire subunit C2. On the basis of the fossils content, three main associations are distinguished (Fig. 6):

Rhaetian (Rh) association – This association is found in the upper portion of the subunit C1. Macroscopically this interval is primarily characterized by the presence of megalodontids. These are extremely abundant, frequently preserved in life position and making very rich bivalve association in which different morphotypes can be recognized. The taxonomic identification of megalodontids specimens is hampered by the difficult to extract the shell from the rock. Nevertheless, at the base of the cycle (lower part of the subtidal interval) megalodontid associations seem oligotypic and are characterized by small-sized specimens, while, in the middle part of the cycle the megalodontid assemblage seems composed by many morphotypes whit a larger average size. (Fig. 7).

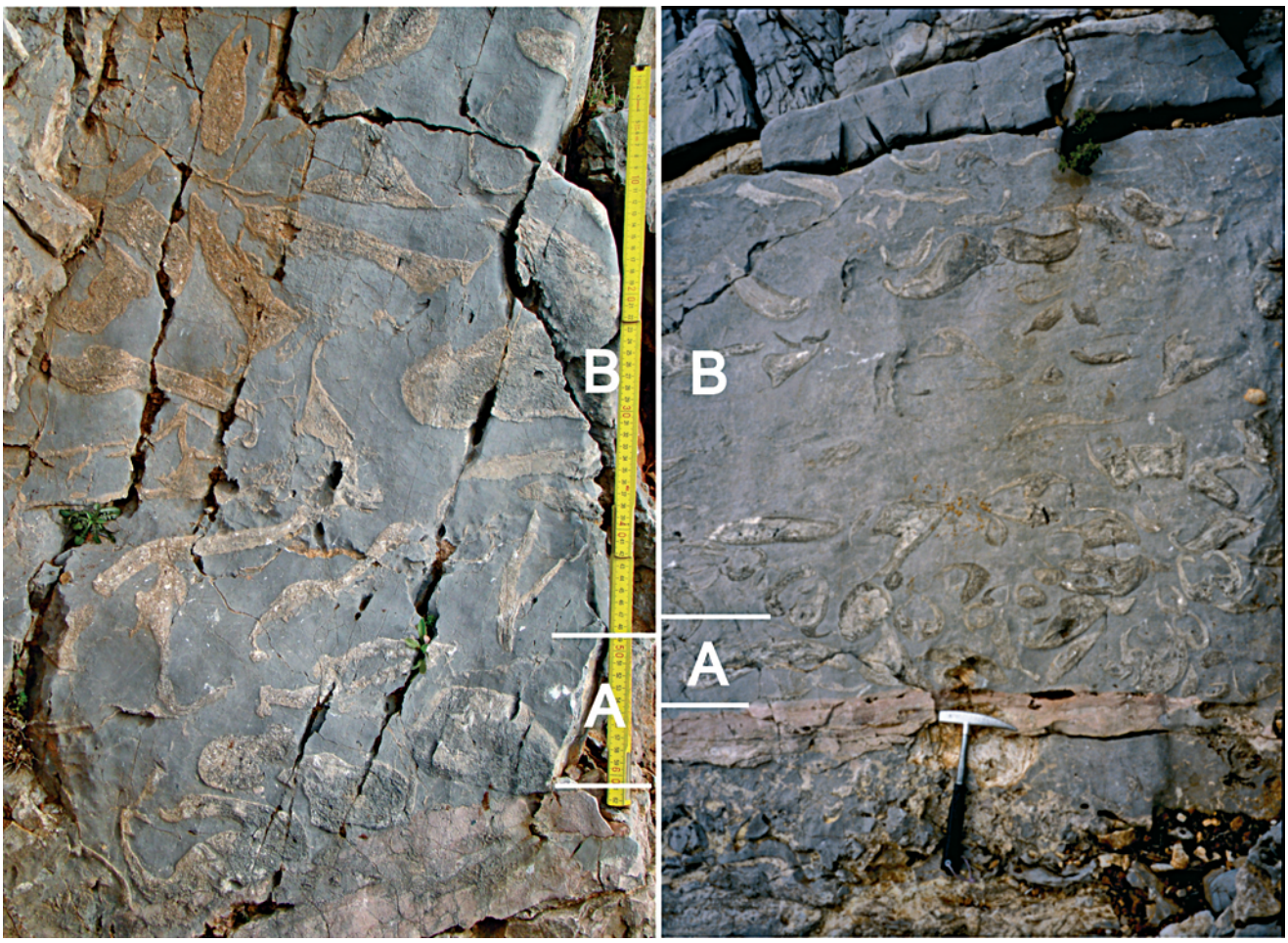

Fig. 7 - Megalodontid assemblage. In the lower part of the subtidal portion (A), small-sized specimens in life position could be observed while in the middle part of the cycle (B) the megalodontid assemblage shows a chaotic arrangement and a larger average size of the specimens.

This stratigraphic interval is also characterized by a rich microfossil content, consisting of small bivalves and gastropods, echinoid spines, several foraminifers and algae. Among the foraminifers there are textulariids, trochamminids, *Aulotortus* spp., and *Triasina hantkeni* Majzon. Dasycladaceae are represented by *Griphoporella curvata* (Gümbel) (Figs 8.1-8.2).

Lower Hettangian association (H1) – This association characterizes the lower portion (130 m) of the subunit C2. Some of the typical macro- and microfossils of the previous interval disappear: starting from the first sample of this interval (sample 26, Fig. 6), megalodontids, *Triasina hantkeni*, *Griphoporella curvata* are absent. The last occurrences of all the previous-listed taxa are recorded near the top of the subunit C1. The association H1 displays a new oligotypic assortment of taxa, in which *Thaumatoporella* spp., *Aeolisaccus dunningtoni* Elliott and small foraminifers as *Siphovalvulina* spp. (Fig. 8.3) prevail. *Thaumatoporella* spp. is very abundant and sporadically forms cushion-like structures (Fig. 8.4). Among the other fossils, there are small bivalves and gastropods, as well as "*Cayeuxia*-like" cyanobacteria. Dasycladales are absent. This microfossil association is typical of lowermost Jurassic (lower Hettangian) limestone deposits (assemblage A-L of Barattolo & Romano 2005) (Fig. 6).

Upper Hettangian association (H2) (Figs 8.5-8) – This association characterizes the middle-upper portion of subunit C2 (100 m) and is marked by the presence of typical Liassic dasycladaceae.

The most representative taxa are *Palaeodasycladus mediterraneus* (Pia), *Tersella alpina* Cros & Lemoine, *Fanesella anae* Sokac, and *Linoporella* sp. (Figs 8.6-8).

The other fossils of this assemblage include: *Aeolisaccus dunningtoni*, *Thaumatoporella* spp., arenaceous foraminifers (primarily siphonous valvulinids), *Duotaxis metula* Kristan, *Lituolipora polymorpha* Gušic & Velic (Fig. 8.5), Rivulariaceae, rare corals, echinoids, gastropods and non-determinable fragments of bivalves. The presence of a level with abundant *Gervillia* shells in the upper portion of the section reveals a close similarity to the Lower Jurassic biofacies in the Tethyan area (i.e. Trento Platform, Italy, Masetti et al. 1998).

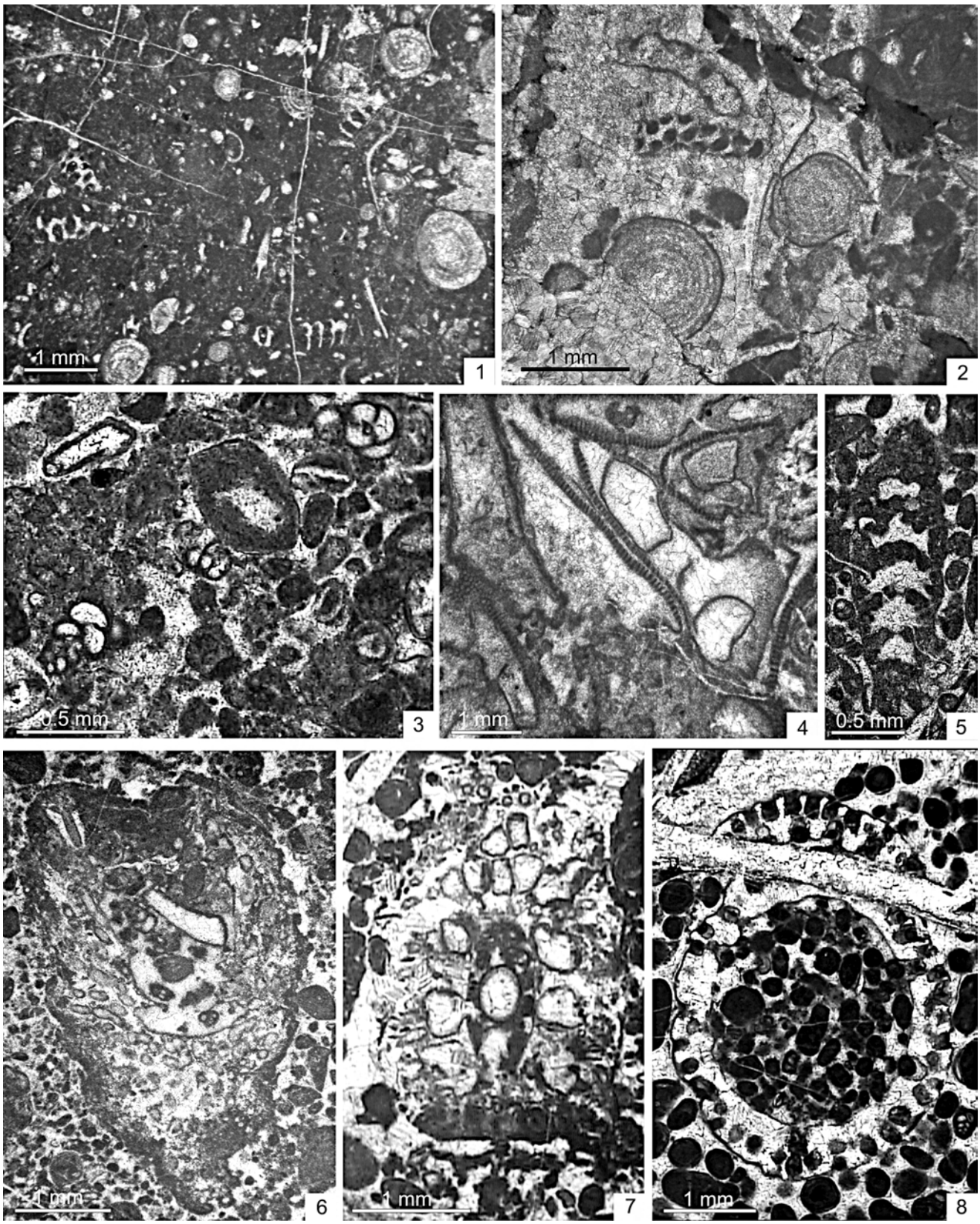

Fig. 8 - Microfossils content of the Messapion section. 1, 2) *Triasina hantkeni* and fragment of *Griphoporella curvata*. Rhaetian, Rh association -sample 22; 3) *Siphovalvulina* cf. *variabilis*. H1 association – sample 66; 4) *Thaumatoporella* spp. with well preserved cellular walls. Hettangian, H1 association -sample 46. 5) *Lituolipora polymorpha*. Hettangian, H2 association - sample 91; 6) *Palaeodasycladus mediterraneus*, oblique section. Hettangian, H2 association - sample 86; 7) *Fanesella anae*, oblique section, Hettangian, H2 association - sample 116; 8) *Tersella alpina*, oblique section of the middle part of the thallus. Hettangian, H2 association - sample 132.

Chronostratigraphic and paleobiologic considerations

De Castro (1991) provides a detailed discussion on the chronostratigraphic distribution of *Triasina hantkeni*. The First Occurrence (FO) of this species is reported in the *Rhabdoceras suessi* zone (Gazdzicki 1983), corresponding to the upper Norian (Dagys & Dagys 1994) or to the lower Rhaetian (Krystyn et al. 2007; Moix et al. 2007). Therefore the FO of *Triasina hantkeni* can be indicated as upper Norian (?) – Rhaetian. In accordance with most of the literature, De Castro (1991) reports the vertical distribution of *Triasina hantkeni* as corresponding roughly to the *Choristoceras marshi* zone, and it does not go beyond the upper boundary of this zone. This datum is also confirmed by recent studies testifying the absence of *Triasina hantkeni* in the sediments referred to the Angulata Limestone (Porto Venere section, Ciarapica 2007).

At the Mt. Messapion the disappearance at 60 m from the base of the section (cycle 34 afterward discussed) of *Triasina hantkeni* and other taxa as megalodontids and *Griphoporella curvata,* are considered Last Occurrences (LO). This interpretation seems supported by sedimentological analysis, since the disappearance of the mentioned taxa (dasycladales, foraminifers and bivalves) is not associated to any facies change. The LO of these taxa is probably related to the end-Triassic biological crisis. The Rh association is interpreted as late Rhaetian in age.

The H1 association is marked by the exclusive occurrence of taxa without a true biostratigraphic value (*Thaumatoporella* spp., *Aeolisaccus dunningtoni,* and small siphonous valvulinid foraminifers) most of which seems also present both in Upper Triassic intervals and in the Lower Jurassic ones (H2 association). According to Barattolo & Romano (2005) these forms may correspond to r-strategy organisms and so the H1 association, represents a post-extinction survival phase, where the decrease in diversity stops and a slight renewal occurs. The H1 association is considered early Hettangian in age.

The H2 association is mainly characterized by the presence of dasycladaleans algae. The First Appearance Datum (FAD) of Jurassic dasycladales marks the lower boundary of this assemblage. In particular the FAD of *Palaeodasycladus mediterraneus* is late Hettangian in age (Barattolo & Romano 2005). On this basis, the unit C is referred to the upper Hettangian, but the upper part of the section (upper part of C2 subunit) may reach the Sinemurian.

From a paleobiogical point of view, H2 association corresponds to the recovery phase, where the taxonomic diversity starts to increase. In this assemblage we register the first occurrence and diversification of dasycladaceae, a decrease of opportunistic taxa (*Aeolisaccus* and *Thaumatoporella*) and the diversification of foraminifers.

In summary, the sequence of the described associations Rh-H1-H2 fits in the typical steps of extinction, survival and recovery phases following a crisis (Fig. 6).

Facies analysis

A detailed facies analysis was performed within the same interval studied from a biostratigraphic point of view. The aim of this approach was the analysis of internal composition and organization of the peritidal cycles.

In the 290 m thick interval studied, 269 elementary cycles were counted. The average thickness of the peritidal cycles falls in a range of 1 to 1.5 m, with sharp erosive upper and lower boundaries for each cycle. Each peritidal cycle is the result of the super-position of the following lithofacies or lithofacies associations: 1) lithofacies a (basal lag); 2) lithofacies association b (subtidal environment); 3) lithofacies association c (inter- to supratidal environment).

In the following paragraphs a description of the identified lithofacies (or lithofacies associations) is given (Fig. 5), as well as a plot of their thickness distribution along the entire section (see Fig. 10). Genetic interpretation is based mainly on investigations of modern tidal flat carbonate environments (Ginsburg & Hardie 1975; Shinn 1983; Hardie & Shinn 1986; Foos 1991; Wright 1994).

Lithofacies a (basal lag)

The lag deposit disconformably lies over the stromatolithic lithofacies; it is laterally discontinuous, and it is made of millimetre to centimetre-sized rip-up clasts of stromatolites, peloids and bioclasts in a mudstone or wackestone matrix (Figs 9.1-2), forming decimeter-thick, often graded beds.

Interpretation - This lithofacies is due to the subtidal reworking of intraclasts. These clasts derive mainly from the erosion and redeposition by storms (Shinn 1983) of desiccated microbial mats during the first marine flooding at the base of the cycle, on top of the laminated lithofacies.

Thickness distribution along the section - The lithofacies a is scarcely represented in the lower part of the section (only in the cycles 3, 13 and 26) (Fig. 10.1). The basal lag is rarely found in the middle and upper part of the Mt. Messapion section, but is commonly present from the middle portion of the section, starting to the 64th cycle. Moreover, the thickness of the basal lag reaches the highest value at the cycle 131. The sporadic occurrence of the basal lag in the lower portion

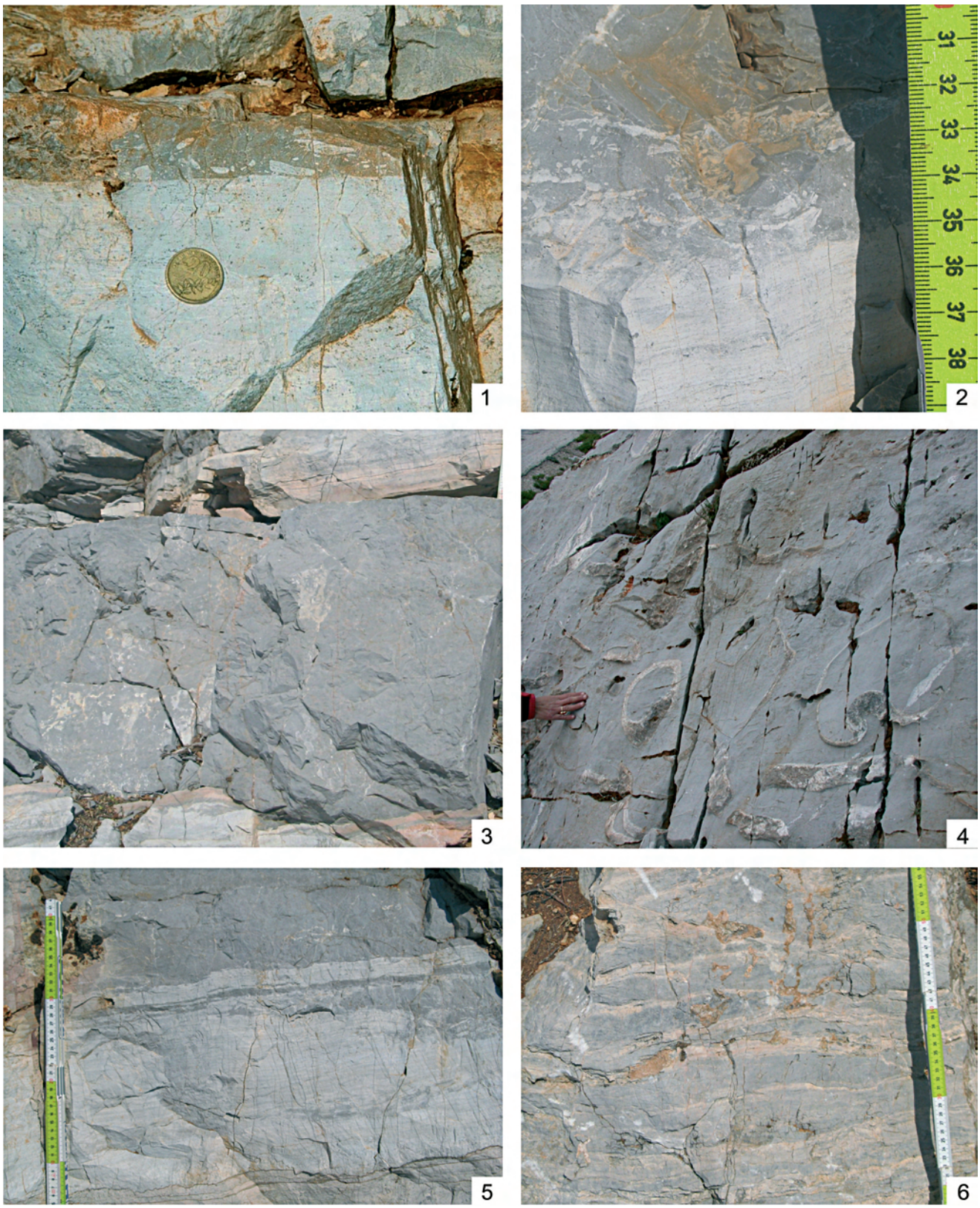

Fig. 9 - Mt. Messapion sedimentary lithofacies. 1, 2) Lithofacies a, basal lag; 3) lithofacies b2-subtidal interval without megalodonts; 4) lithofacies b1-subtidal interval with megalodontids; 5) lithofacies c1-LLH stromatolite without desiccation structures; 6) lithofacies c2-LLH stromatolite with desiccation structures.

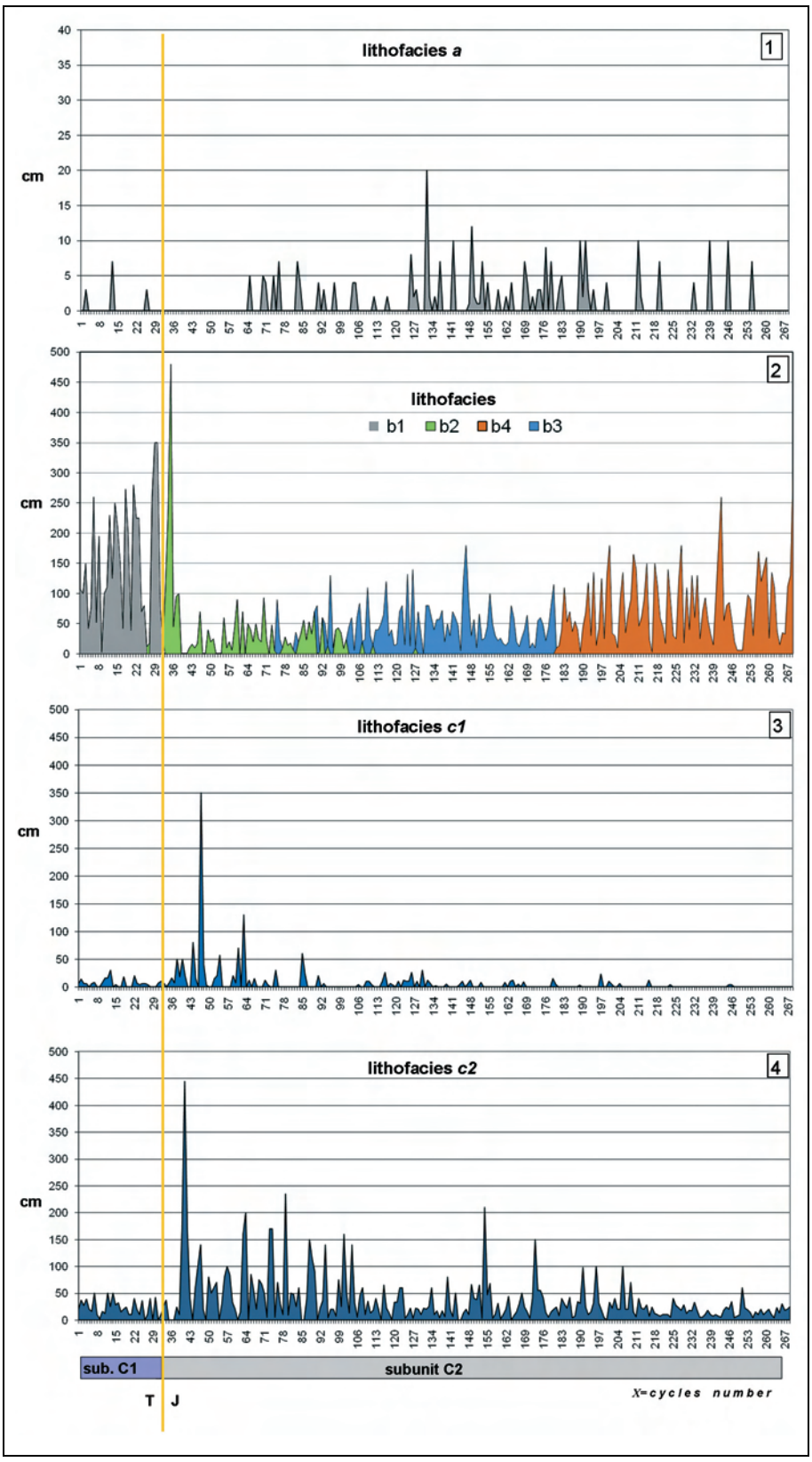

Fig. 10 - Diagrams showing the thickness distribution of the main lithofacies along the section. 1) lithofacies a; 2) lithofacies b1, b2, b3, b4; 3) lithofacies c1; 4) lithofacies c2.

of the section (subunit C1) could be related to several factors:

(i) The presence of a marginal area tending to develop a wave-resistant rim that protects the sediments of the platform interior, thus weakening the storm action (reworking of the substratum-basal lag). Flügel (2002), in an exhaustive study on the patterns of Phanerozoic reefs, reports that the global reef volume at the T/J boundary exhibits the most remarkable collapse of the Phanerozoic, in terms of both absolute and normalized values; 37 reef sites are listed in the Rhaetian and only four occurrences for the Hettangian testify a wide-

spread change in the nature and composition of the platform margin area. The Late Triassic was characterized by rimmed platform margins frequently represented by wave-resistant buildups (coral-sponge reef: Sicily, Carnian Prealps, Pendeoria area and Hydra) while the Lower Jurassic platforms are referable to an open shelf rimmed by oolitic shoal marginal systems. The decline of the reef communities at the T/J boundary probably implies also the transition from a back reef environment characterized by medium-low energy to an open environment more directly exposed to wave- or storm wave action.

(ii) The occurrence of the basal lag is a direct expression of the frequency of the storm events. In turn, this would depend on the climatic conditions during Late Triassic times.

(iii) High sedimentation rate. The carbonate production assured the quick burial of the supratidal layers, preventing the reworking of the substrate (Masetti et al. 1985).

In the stratigraphic interval in which the basal lag is frequently recorded (from cycle 95 to 165) we can consider opposite causes of the previously discussed ones.

– Absence of a wave-resistant rim that protects the sediment of the platform interior, weakening the wave and storms action (reworking of the substrate – basal lag).

– The frequency of the basal lag is directly related to the frequency of the storm events. This is a characteristic of the climatic condition during earliest Jurassic times.

– Low sedimentation rate. The carbonate production is insufficient to assure the burial of the supratidal layers and the substrata is exposed to the action of the wave and storms (Masetti et al. 1985).

Lithofacies association b (subtidal environment)

The lithofacies association b (Figs 9.3-4) represents the most prominent interval in each cycle and made of deposits and processes peculiar of subtidal environments that opened in front of the supratidal area of the tidal flat. Inside this subtidal domain, which according to the present physiographic models in the Messapion section corresponds to a lagoon, it is possible recognize four further lithofacies representing sub-environments characterized also by different paleontological content:

(*b1*) Metre-thick bioturbated beds of wackestone-packstone with megalodontids and foraminifers. Other fossils are present: gastropods, *Thaumatoporella* spp., calcareous algae. Most of the grains are bioclasts, rare ooids and other coated grains are also present. The widespread bioturbation, at least partially produced by the megalodontid fauna, effaces all sedimentary structures. This lithofacies characterizes the lower portion of each cycle in the subunit C1.

(*b2*) Thick-bedded wackestone-packstone, without megalodonts but containing *Thaumatoporella*, *Aeolisaccus,* and *Siphovalvulina*. These taxa are the only microfossils characterizing this lithofacies: abundant *Thaumatoporella* is commonly found, sometimes making centimetres cushion-like structures. Lithoclasts, ooids and coated grains are rare or absent. The lithofacies b2 characterizes the lower portion of each cycle in the subunit C2 (lower part).

(*b3*) Wackestone-packstone with oncoids. This lithofacies is characterized by the same microfossil content as lithofacies b2, i. e. *Siphovalvulina* spp., *Thaumatoporella* spp., *Aeolisaccus dunningtoni*, but dasycladales algae are present as well. Oncoids of 0.5-1.5 cm in diameter, with an agglutinated bioclastic nucleus and microbialitic envelope are present. This lithofacies characterizes the middle part of the subunit C2.

(*b4*) Bedded packstone-grainstone without evident current structures. This grain-supported lithofacies is characterized by ooids and bioclasts; fossils include foraminifers, dasycladales and fragments of bivalves and gastropods. This lithofacies is characteristic of the upper part of the subunit C2.

Interpretation – Lithofacies b is interpreted to reflecting a subtidal, lagoonal setting, and its several sub-environments, each characterized by different depositional processes. In the more sheltered areas quiet water conditions dominate, the sediment settling prevails and the bioturbated mud is deposited (Lithofacies b1 and b2). On the contrary, the high water turbulence near the tidal inlets leads to the deposition of laminated oolitic and bioclastic sand, modelled by traction currents flowing both in a lower or upper flow regime (Lithofacies b3 and b4).

Thickness distribution along the section (Fig. 10.2) – The lithofacies b occurs along the entire section. This lithofacies ranges from centimetres- to metres-scale and the highest thickness is recorded in the lower portion of the section (subunit C1 from the cycle 1 to the cycle 37). Starting from cycle 38 up to the 94, lithofacies b shows thickness values below 1 m. The thickness of this lithofacies moderately increases after the cycle 95, reaching 1.5-2 m after the cycle 190. The subtidal interval of the cycles in the upper portion of the section shows thicknesses similar to the lower portion.

The thickness changes of the lithofacies b well fit with the distribution of the four different lithofacies b1-b4. The interval characterized by lithofacies b1 corresponds to the maximum value of the recorded thickness (subunit C1, cycles 1 to 31). Lithofacies b2 initially is characterized by high thickness (from cycles 32 to 37), but later on it is associated with low thickness (cycles 38-100), similarly to lithofacies b3 (from cycle 36 to

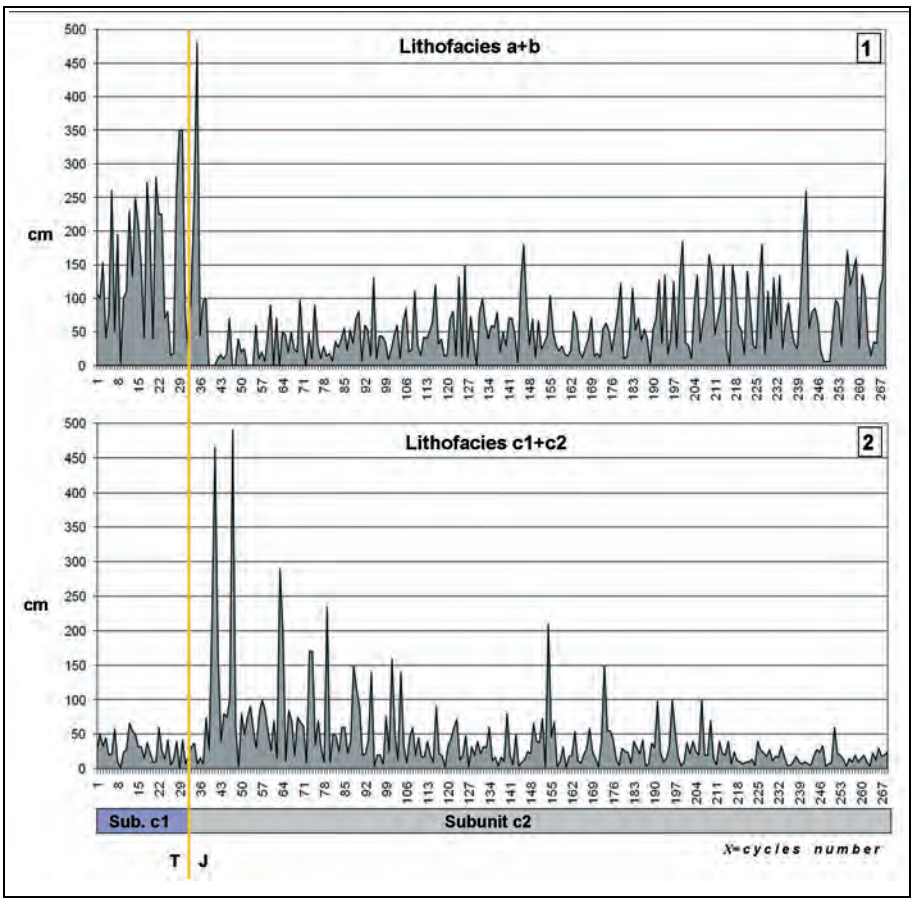

Fig. 11 - Diagrams showing the thickness distribution of two group of lithofacies along the section. 5) Lithofacies a and b; 6) lithofacies c1 and c2.

190). Lithofacies b4 seemingly corresponds to the restoration of the initial thickness value (the subtidal intervals of the cycles from 191 to 269 show values ranging from 1.5 to 2 m).

Lithofacies association c (inter-supratidal environment)

The lithofacies association c represents the shallowest stage of the cycle deposited in the inner part of the tidal flat. It is possible to distinguish two different lithofacies: c1 (Figs 9.1-9.5) and c2 (Fig. 9.6). Both lithofacies are made of stromatolitic bindstone and differ on the presence or absence of subaerial structures.

The lithofacies *c1* (LLH stromatolites without desiccation structures) is made of microbial stromatolite, light grey, without fenestral pores or other structures related to a sub-aerial exposure. The lamination is generally planar or gently undulating, sometimes wrinkly, and irregularly alternates with centimetre-thick micritic horizons (Fig. 9.6).

The lithofacies *c2* (LLH stromatolites with desiccation structures) is made of microbial stromatolite, light grey, pinkish, with laminoid and irregular fenestrae, incipient shrinkage cracks (Fig. 9.1-9.5). The lamination is wrinkled or sometime planar. Crinkly lamination with fenestral pores indicates episodic exposure and desiccation.

Interpretation of lithofacies c1 and c2 – Both lithofacies record the trapping by microbial mats of fine-grained sediment settled down from the water after a storm in the inner portions of the tidal flat. The preservation of fenestral pores via early diagenetic cementation and the presence of sheet cracks, suggest a supratidal environment, while their absence indicates an intertidal environment.

Thickness distribution along the section (Figs 10.3-10.4) – The lithofacies c1 represents the intertidal interval of the cycle. In some parts of the section this lithofacies is present only sporadically and seems to form clusters between the cycle 34 and the 62. In the same interval the basal lag (lithofacies a) is absent (from the cycle 27 to the 63, Fig. 10.1) and the subtidal intervals of the cycles are thin (less than 1 m for cycles 36-63, Fig. 10.2) and exclusively represented by lithofacies b2 (Fig. 10.3).

The lithofacies c2 reaches the maximum thickness at the cycle 39 and gently decreases in thickness starting from the cycle 40 to 103. (Fig 10.4) The maximum values of lithofacies c2 are commonly associated with the subtidal lithofacies b1 and with a higher thickness in the intertidal lithofacies c1.

After the description of composition, thickness and distribution of each lithofacies, it is possible to

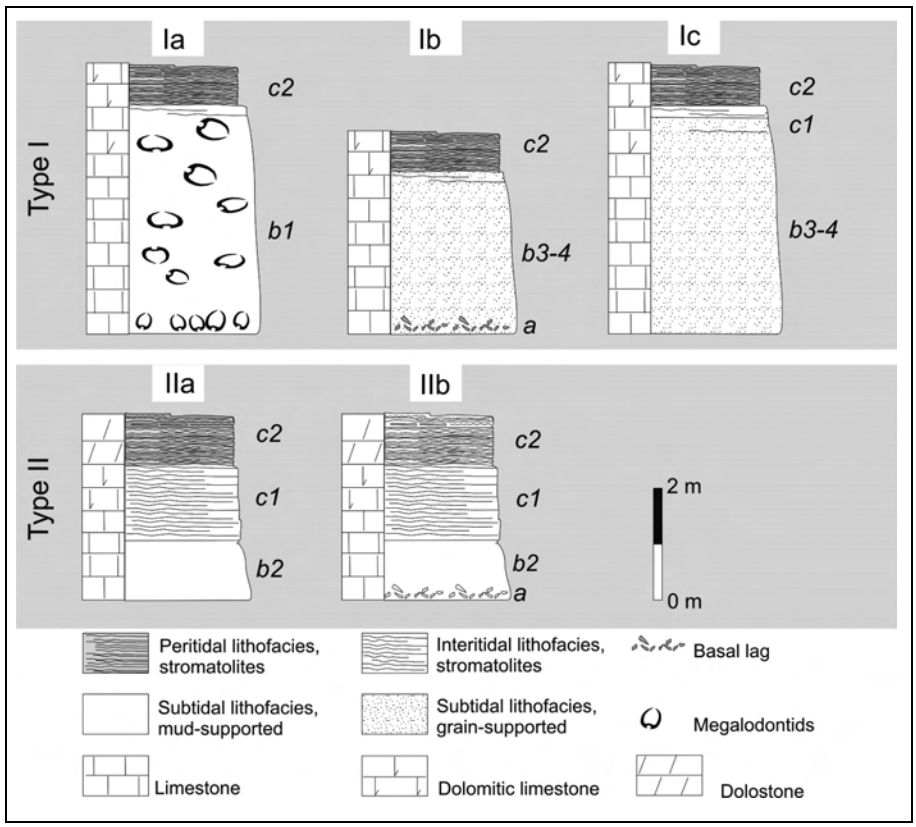

Fig. 12 - Main cycle types recognized in the studied interval of the Mt. Messapion section. Type I (Ia-Ib and Ic): constant presence of thick and bioturbated subtidal interval (with or without megalodontids), supratidal interval and sporadic presence of basal lag. Type II (IIa-IIb): subtidal interval with sporadic presence of basal lag, thick intertidal and supratidal lithofacies.

analyze also the variation of lithofacies groups along the studied interval (Figs 11.1-11.2). The lithofacies are grouped using genetic criteria: lithofacies linked to subtidal environment (a and b1-4 lithofacies, Fig 11.1) and lithofacies characterized by common development of inter and supratidal environment (lithofacies c1 and c2, Fig 11.2). The diagrams in Figs 11.1-2 display the variation of these two lithofacies group. The two curves (a+b) and (c1+c2) are complementary. The first one rises up until the 37th cycle and then decreases. The (c1+c2) curve increases exactly starting from the cycle 37. From cycle 37 to 105 the curve (a+b) exibits lower values, while curve (c1+c2) is characterized by much higher values. After the cycle 105 the curve (a+b) gradually increases while the curve (c1+c2) gradually decreases. Therefore, the main thickness change is observed at cycle 37. After this stratigraphic point the cycles result composed by a thin subtidal portion subordinate to the inter and supratidal one.

Elementary cycles and their vertical organization

Along the section, the above-described lithofacies are vertically stacked in different ways to form several cycles, each one corresponding to a minor variation inside the same shallowing- upward sedimentary trend, which corresponds to a progradational phase of a tidal flat system. Based on the ratio between subtidal and inter and supratidal lithofacies, two main cycle types (I and II) have been recognized. Inside these cycle types, further variants have been identified according to the presence of different lithofacies.

The two main types of cycles are as follows:

Type I (Fig. 12) is composed of sporadic presence of the basal lag (lithofacies a) and the constant presence of thick and bioturbated subtidal interval (lithofacies association b), whereas the intertidal interval (lithofacies c2) is very thin or absent. The Type I cycle can be subdivided into three further subtypes:

I.a – The cycle is made only of lithofacies b1 or b2 and c2. The basal lag is absent and the transition between the subtidal and supratidal interval is sudden and lacks the peritidal lithofacies c1.

I.b – The basal lag characterizes the base of the cycles; lithofacies b3 or b4 of the subtidal interval is capped by the supratidal lithofacies c2.

I.c – The cycle is characterized by the absence of the basal lag and made of subtidal lithofacies b3-b4; sometime a thin peritidal lithofacies c1 is covered by the supratidal lithofacies c2.

Type II. This cycle type is made of a basal lag, followed by a thin subtidal interval (lithofacies b2) grading upward to a very thick peritidal lithofacies c1. The cycle is capped by the supratidal stromatolites of the lithofacies c2. Inside the Type II two subtypes, II.a and II.b, can be distinguished based on the presence of lithofacies a (Fig. 12).

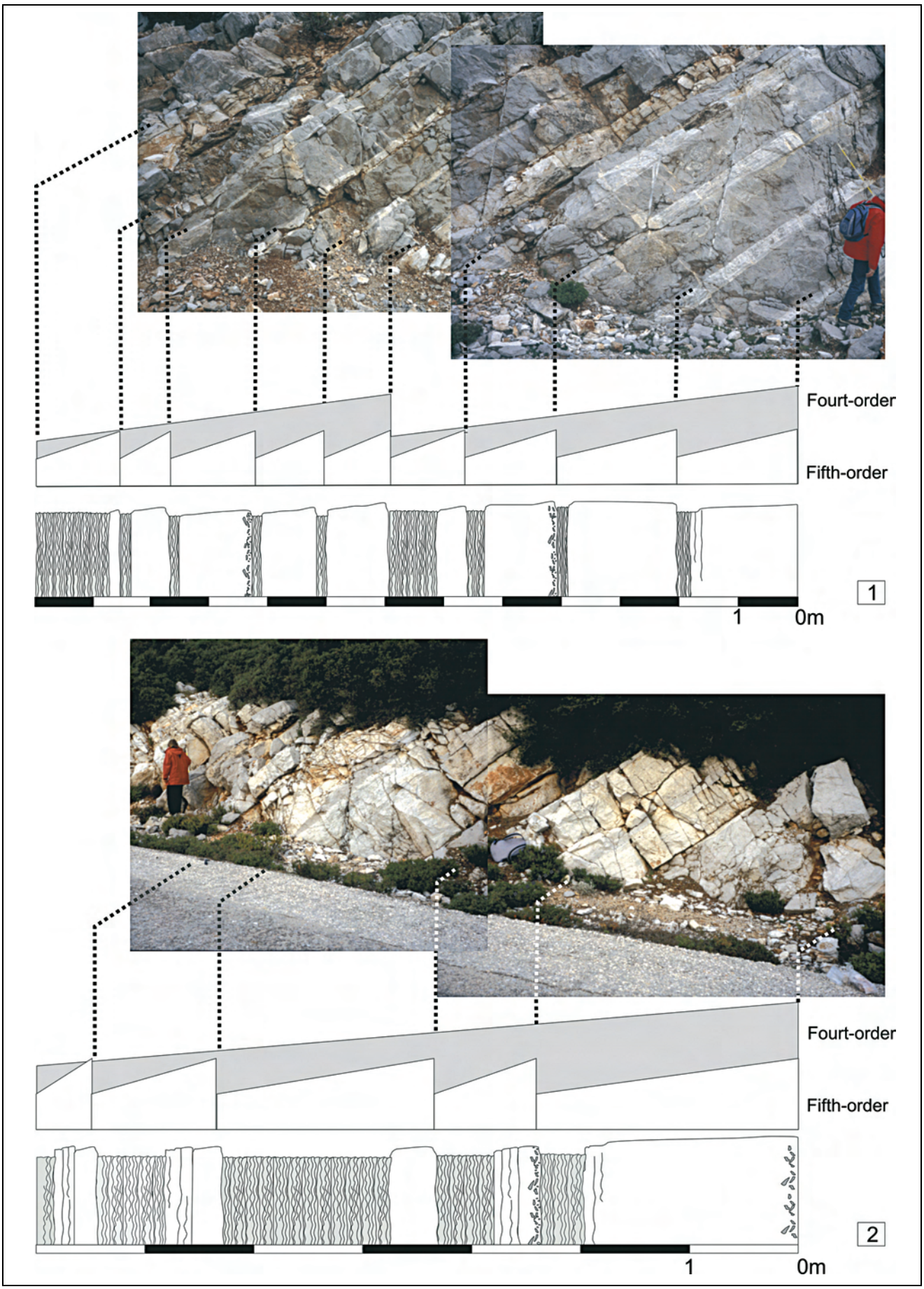

Fig. 13 - Different types of cycle bundles. 1) Group of four-five Type I cycles; 2) group of four-five Type II cycles. Legend in Fig. 11.

The stacking pattern of the lithofacies (elementary cycles) and their grouping reveals the existence of a hierarchical organization along the entire measured section. The shallowing-upward cycles are grouped in bundles of four-five elementary cycles. Depending on the constituent types of the elementary cycle (I or II types), the bundles show a very different aspect and thickness but always display the same shallowing-upward trend (Figs 13.1-13. 2). The bundle illustrated in Fig. 13.1, is composed of a group of four or five Type I cycles and characterizes the subunit C1 and first metres of subunit C2 (Fig. 13).

The second typology of bundle (Fig. 13.2) is composed of a group of four or five Type II cycles; the elementary cycles are mainly represented by laminated lithofacies c1-c2, increasing its thickness inside the bundle from the bottom to the top. This bundle typology characterizes the middle portion of the section from m 65 to 200 (Fig. 14).

This hierarchic organization suggests an allocyclic control for the cyclothemic deposition of the Messapion section; each elementary cycle is considered as the record of a fifth order cyclicity grouped into fourth order bundles. This elementary organization of the cycles into bundles of higher order is confirmed by preliminary statistical analysis and by the field work. The cyclicity of the Mt. Messapion section was already directly registered on the field. However, despite the field evidence, the cyclic signal still requires an accurate statistical processing in order to understand the meaning and value of its controlling processes (Milankovitch cycles, climatic control, etc.).

Discussion

The Mt. Messapion section clearly demonstrates that the T/J boundary had only minor or negligible evidences in the local shallow water environment. The peritidal cyclicity persists along the entire section, with small modifications in its internal organization, affecting only the supratidal/subtidal ratio and thus the average depositional depth. A comparison of the variation in cycle typology across the section and the fossil content reveals a clear detachment between the paleontological turnover (disappearance of megalodontid communities and microfossil assemblages) and the distribution of the different cycle typologies (Fig. 14).

The shift from Type I to Type II cycles occurs about 13.4 m above the T/J boundary and manifests in a substantial decrease in thickness of subtidal intervals in each cycle; as a whole, the thickness of the subtidal intervals of the basic cycles along the whole section is characterized by a rhythmic thickening (Type I cycles)

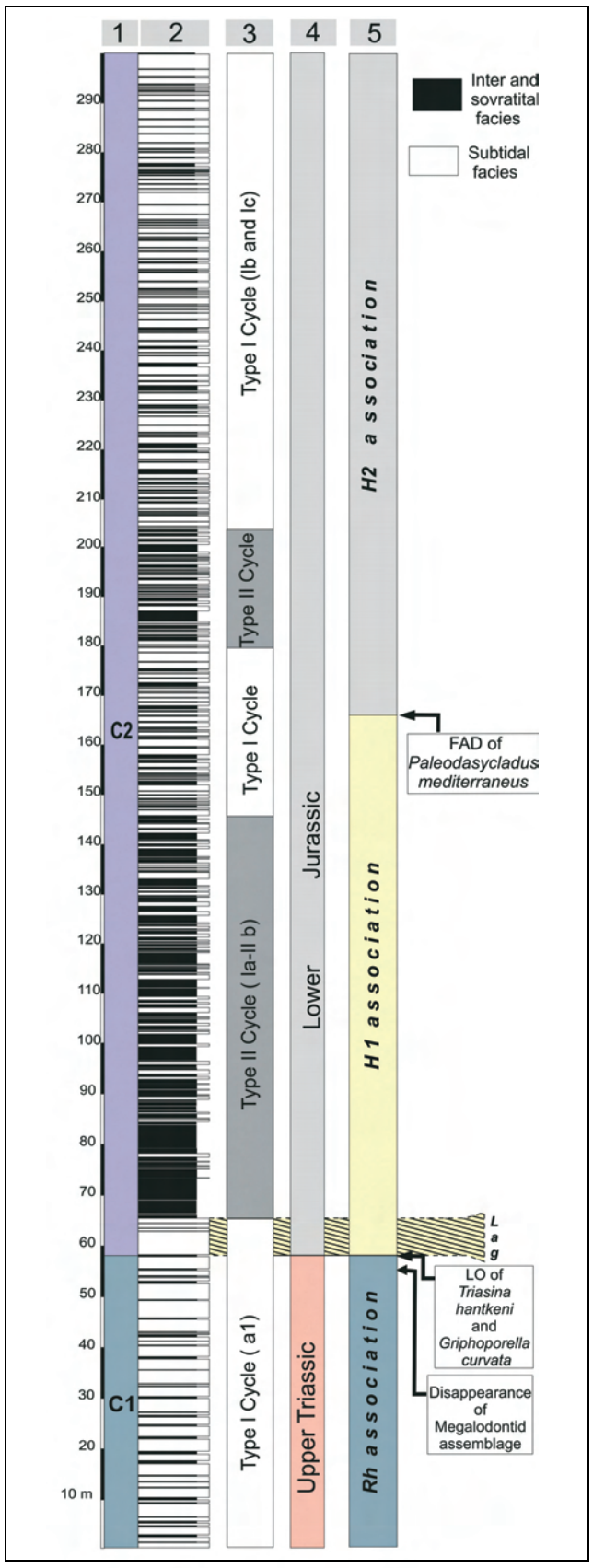

Fig. 14 - Distribution and correlation of stratigraphic and biostratigraphic data of Mt. Messapion section. 1) Unit subdivision; 2) stratigraphic log; 3) type (I-II) cycles distribution; 4) chronostratigraphic interpretation and 5) paleontological associations. A lag between the change in the paleontological content and cyclic organization can be observed.

and thinning (Type II cycle), just like a playing a squeezebox or accordion (Fig. 14).

To understand the driving force of this rhythmic sedimentation, it is necessary to recall that two different models are proposed to explain the cyclic pattern observed in Upper Triassic peritidal platform: the classic autocyclic model (Goldhammer et al. 1990; Satterley 1996; Satterley & Brandner 1995; Enos & Samankassou 1998) and the allocyclic model (Fischer 1964; Schwarzacher & Haas 1986; Haas 1994, 2004; Balog et al. 1997; Cozzi et al. 2005). After 40 years of researches a consensus has still not been reached on the periodic versus random origin of the peritidal cyclicity.

The unravelling between auto- versus allocyclic interpretation of cyclothemic section cropping out at Mt. Messapion is beyond the scope of this paper. However, the thinning of the subtidal intervals within each cycle, recorded by the shift between Type I to Type II cycles, testifies the substantial decrease of the accommodation space available. In the autocyclic model, the accommodation space, during a steady relative sea-level, is the result of the interaction between subsidence and sedimentation rate.

Since in the autocyclic model the subsidence rate is considered constant, the variation of the accommodation space available depends only on the sedimentation rate. If the sedimentation rate is not much higher than the rate of subsidence, the time needed to fill up the available space will be longer and so the time in which the subsidence can influence the accommodation space itself. On the contrary, a high sedimentation rate, filling up quickly the accommodation space, cancels or reduces the effect of subsidence. In summary, a high rate of sedimentation in the autocyclic model minimizes the effect of subsidence and produces a thinner cycle compared with that related to a relatively low rate of sedimentation.

In the allocyclic model a decrease in the accommodation space (transition from Type I to II cycle) can be considered as result of:

1) A fall of the sea level coupled with a constant or lower rate of sedimentation.

2) A rise of the sea level coupled with a higher rate of sedimentation.

According to the recent literature (e.g. Hallam & Wignall 1999; Tanner et al. 2004), the sea-level underwent a fall in the upper Rhaetian and began to rise in early Jurassic (Hallam 1981; McRoberts et al. 1997; Hallam & Wignall 1999; Hesselbo et al. 2004)

Evidence of a sea level rise are reported in Germany and in northern Frankonia (Bavaria), where marine Hettangian deposits overlying the fluvial sandstones infill channels incised into upper Rhaetian marine strata (Bloos 1990). Both in the Northern and Southern of Europe (Hallam 1991, 1995; Hallam & Goodfellow 1990) a similar pattern of successive sea-level fall and rise can be inferred; a clear end-Triassic regressive pulse can be recognized in the Danish Basin (Bertelsen 1978), while both in southern Sweden and NW Poland the upper Rhaetian (Bertelsen 1978) is missing and there is an unconformity at the base of the Jurassic. In the Northern Calcareous Alps of Austria (Hallam 1997), widespread emergence at the end of the Triassic is recognized.

Galli et al. (2007) reported the occurrence of a transgressive phase at the base of the Hettangian stage (Malanotte Formation, Lombardy, Italy); Haas & Tardy-Filácz (2004) signalled a deepening trend in the early Hettangian basin deposits of the Cosvàr Fm. (Transdanubian Range, Hungary). In conclusion, the hypothesis 1, providing a fall of the sea level for to explain the transition between Type I to Type II cycles, is in disagreement with the literature data.

If we interpret the deposition of the Type II cycle as the result of a transgressive trend, according to hypothesis 2, we must assume an increase in the sedimentation rate.

Whereas the siliciclastic systems depend on external sediment supply, for carbonate systems the ability to grow upward and produce sediment is an intrinsic property. Haas & Tardy-Filácz (2004) and Galli et al. (2005, 2007) suggest that the carbonate factory seems to reflect reduced productivity in connection with the Triassic/Jurassic "boundary event". The T/J boundary is marked by one of the biggest five extinctions of the Phanerozoic, when 48% of marine invertebrate genera disappeared (Sepkoski 1996), among them many cephalopods, bivalves, gastropods, brachiopods and reef organisms (Hallam 1990; Flügel 2002). Most of these taxa are important carbonate producers and their disappearance from the fossil record is considered the cause of the carbonate factory crisis.

At the Mt. Messapion section, the transition from Type I to Type II cyclicity is interpreted as an increase of the sedimentation rate. This can be explained assuming that the mass extinction at the T/J boundary caused the switching off of the Upper Triassic carbonate factory (with corals, bivalves etc.) following by a change of the carbonate producer; this new carbonate production play went on, and probably raised.

In the lowermost Hettangian deposits of the Mt. Messapion section, the subtidal intervals are represented by micritic sediments with a rare skeletal grain component. Some micritic sediments can be transported from marginal areas to the inner platform, but they are principally produced *in situ* by degradation of calcareous green algae, whiting, chemical precipitation and microbially-induced precipitation (M factory sensu Schlager 2005). These carbonate producers (green algae, blue-green algae, cynobacteria, etc) are testified

in the fossil record often only by the products of their activity or degradation (micrite), while a direct control of their presence and abundance is hampered by the absence of fossilizable hard parts. These biogenic carbonate producers can be probably interpreted and identified as *r* strategist organisms (Hottinger 1983; Barattolo & Romano 2005) characterizing the first steps of post-extinction recovery time and probably present also in the B assemblage of Mt. Messapion section.

Both the model, autocyclic and the allocyclic hypothesis 2 (see above) providing an increase of the sedimentation rate for to explain the I-II Type cycle transition, are suggestive but needs further detailed studies (sedimentological, paleoecological, micropaleontological).

Conclusively, at the Mt. Messapion, neither models (autocyclic or allocyclic) result completely satisfactorily or in agreement with the bibliographic data.

Conclusion

In this paper we present the first integrated stratigraphic study performed on an expanded section of Upper Triassic - Lower Jurassic limestones. During the last years, many multidisciplinary investigations, focused on slope and basinal deposits, obtained new integrated stratigraphic data helpful for the identification of the latest Triassic-earliest Jurassic events. On the contrary, knowledge on the T/J boundary events in shallow water successions is much less advanced, either for the scarcity of sections studied in detail, or for the very poor fossil content characterizing the lower Hettangian platform deposits. The main results of this study of the Mt. Messapion section are summarized in the following five points.

i) A detailed facies analysis performed along a 290 m thick stratigraphic interval (60 m above the T/J boundary and 230 m below it) allowed the recognition of peritidal cycles. Five different elementary cycles are described and their distribution along the section is given.

ii) The T/J boundary is identified by (1) the last occurrence of *Triasina hantkeni* Majzon, (2) the abrupt disappearance of megalodontid faunas and (3) the appearance of Jurassic microfossil associations. The persistence of the facies and the lack of any major paleoenvironmental change across the T/J boundary offered also the opportunity to study in detail the distribution of the shallow water microfossils.

iii) The paleontological reorganization at the T/J boundary is sudden and not controlled by any facies change; it seems to produce no evident modification in the vertical stacking pattern of the cycles.

iv) The relationship among cyclicity, sea level change and carbonate producers is discussed.

The effects of evolution on the basic functioning of the carbonate system, on loci and rates of carbonate production, and on facies distribution, remain unresolved questions of this work, because the complexity of the carbonate system needs a detailed knowledge of any single process involved in the system (biological evolution, sea level change, sedimentation mechanisms, etc.)

v) The rhythmical superimposition of the cycles and their hierarchical grouping suggest an allocyclic control. Composite Milankovitch-type, glacio-eustatic fluctuations seem to be the only mechanism able to generate the high-frequency multi-hierarchic pattern described at Mt. Messapion. Assuming as a working hypothesis that the Mt. Messapion section represents the sedimentary record of an allocyclic composite Milankovitch-type, glacio-eustatic forcing, the count of cycles could represent a powerful tool to have a precise evaluation of the time span involved in the succession of events at the T/J boundary.

This paper may represent only the first step of a more exhaustive work on the T/J boundary in shallow water environment. We consider the study of this environment a key to understand the event succession occurred during this crucial time interval, since the carbonate platforms represent a potentially complete and expanded archive (compared to the often condensed basinal environments), in which the cause-effect relations between physical and biological events can be reconstructed.

Acknowledgments. We are grateful to Dr. Anastasios Mavrides (IGME -Athens) for calling our attention to the Mt. Messapion section. We would like to thank the numerous colleagues who have contributed to the mapping and sampling of the stratigraphic section during several field trips, especially Dr. Luca Paolillo, Dr. Antonio Giordano and Miss Ilaria Roghi. The authors wish to thank the Direction of IGME (Athens) for field work permissions. Many thanks to J. Palfy and F. Jadoul for the critical review of the manuscript and their useful comments and suggestions. This research was supported by the M.I.U.R, Italy (PRIN 2005, Local Project Manager, Prof. D. Masetti).

REFERENCES

Balog A., Haas J., Read J.F., Coruh C. (1997) - Shallow marine record of orbitally forced cyclicity in a Late Triassic carbonate platform, Hungary. *J. Sediment. Res.,* 67(4):661-675, Tulsa.

Barattolo F. & Romano R. (2005) - Some bioevents at the Triassic-Liassic boundary in the shallow water environment. *Boll. Soc. Geol. Ital.,* 124: 123-142, Roma.

Bassoullet J.P. (1997a) - Les grands foraminifères. In: Biostratigraphie du Jurassique ouest-Européen et Méditerranéen (Coord. E. Cariou and P. Hantzpergue). *Mém. Centres Rech. Explo.-Prod. Elf Aquitaine*, 17: 294-304, Pau.

Bassoullet J.P. (1997b) - Algues dasycladales. Distribution des principales espèces. In: Biostratigraphie du Jurassique ouest-Europèen et Méditerranéen (Coord. E. Cariou and P. Hantzpergue*), Mém. Centres Rech. Explo.-Prod. Elf Aquitaine*, 17: 339-341, Pau.

Berra F., Delfrati L. & Ponton M. (2007) - Dolomia Principale Carta Geologica d'Italia 1:50.000 - *Quaderni del servizio Geologico d'Italia- Catalogo delle Formazioni* - Serie III, Vol. 7 - Fasc. VI: 63-72, Roma.

Bertelsen F. (1978) - The Upper Triassic-Lower Jurassic Vinding and Gassum Formations of the Norwegian-Danish Basin. *Danmarks Geologiske Undersogelse,* Series B3: 1-26, Copenhagen.

Bloos G. (1990) - Sea level changes in the Upper Keuper and in the Lower Lias of Central Europe. *Cahiers de l'Institut Catholique,* Serie Scientifique, 3: 5-16, Lyon

BouDagher-Fadel M.K. & Bosence D. (2007) - Early Jurassic benthic foraminiferal diversification and biozones in shallow-marine carbonates of western Tethys. *Senckenbergiana lethaea,* 87: 1-39, Frankfurt.

Bosellini A. (1967) - La tematica deposizionale della Dolomia Principale (Dolomiti e Prealpi Venete). *Boll. Soc. Geol. Ital.*, 86: 133-169, Roma.

Bosellini A. & Hardie L.A. (1988) - Facies e cicli della Dolomia Principale delle Alpi Venete: *Mem. Soc. Geol. It.*, 30: 245-266, Roma.

Carras N. & Georgala D. (1998) - Upper Jurassic to Lower Cretaceous Carbonate Facies of African Affinities in a Peri-European Area: Chalkidiki Peninsula, Greece. *Facies*, 38: 153-164, Erlangen.

Celet P., Clément B. & Ferrière J. (1988) - Evolution géodynamique de la plate-forme pélagonienne au Mésozoïque. 3rd Congress of the Geol. Soc. of Greece, Athens, 1986, *Bull. Geol. Soc. Greece*, 20(1): 215-222, Athens.

Celet P. & Ferrière J. (1978) - Les Hellénides internes: Le Pélagonien. *Eclogae geol. Helv.*, 71(3): 467-495, Basel.

Chiocchini M., Farinacci A., Mancinelli A., Molinari V. & Potetti M. (1994) - Biostratigrafia a foraminiferi, dasicladali e calpionelle delle successioni carbonatiche mesozoiche dell'Appennino Centrale (Italia). In: Mancinelli A. (Ed.) - Biostratigrafia dell'Italia Centrale. *Studi Geologici Camerti*, Vol. Spec. (1994): 9-128, Camerino.

Ciarapica G. (2007) - Regional and global changes around the Triassic-Jurassic boundary reflected in the late Norian-Hettangian history of the Apennine basins. *Palaeogeogr. Palaeoclim. Palaeoecol.*, 244: 34-51, Amsterdam.

Ciarapica G. & Passeri L. (1998) - Evoluzione paleogeografica degli Appennini. *Atti Tic. Sc. Terra*, 40: 233-290, Pavia.

Ciarapica G. & Passeri L. (2002) - The paleogeographic duplicity of the Apennines. *Boll. Soc. Geol. Ital.* Vol. Spec. 1: 67-75, Roma.

Ciarapica G. & Passeri L. (2005) - Ionian Tethydes in Southern Apennines. In: Finetti I.R. (Ed.) - CROP - Deep Seismic Exploration of the Mediterranean Region. Atlases in Geoscience, 1: 209-224, Elsevier, Amsterdam.

Cozzi A., Hinnov L.A. & Hardie L.A. (2005) - Orbitally forced Lofer cycles in the Dachstein Limestone of the Julian Alps (northeastern Italy). *Geology*, 33(10): 789-792, Boulder.

Dagys A.S. & Dagys A.A. (1994) - Global correlation of the terminal Triassic. *Mém. Géol.*, 22: 25-34, Lausanne.

De Castro P. (1991) - Mesozoic. In: Barattolo F., De Castro P. & Parente M. (Eds) - 5th International Symposium on Fossil Algae. Field Trip Guide- Book., pp. 21-38, Giannini, Napoli.

Demicco R.V. & Hardy L.A. (1994) - Sedimentary structures and early diagenetic features of shallow marine carbonate deposits., *SEPM (Society for Sedimentary Geology)* Atlas Series, 1, 265 p., Tulsa.

Dercourt J. (1972) - The Canadian Cordillera, the Hellenides and the sea-floor spreading theory. *Canad. J. Earth Sci.*, 9: 709-743, Kelowna.

Dercourt J., Zonenshain L.P., Ricou L.E., Kazmin V.G., Le Pichon X., Knipper A.L., Grandjacquet C., Sborshchikov I.M., Boulin J., Sorokhtin O., Geyssant J., Lepvrier C., Biju-Duval B., Sibuet J.-C., Savostin L.A., Westphal M. & Lauer J.P. (1985) - Présentation de 9 cartes paléogéographiques au 1/20.000.000 s'étendant de l'Atlantique au Pamir pour la période du Lias à l'Actuel. *Bull. Soc. Géol. France*, (8), t. I, n. 5: 637-652, Paris.

Dercourt J., Ricou L.E. & Vrielynck B. (1993) - Atlas Tethys paleoenvironmental maps. *CGMW,* 307 p., 14 maps, 1 pl., Paris.

Enos P. & Samankassou E. (1998) - Lofer cyclothems revisited (Late Triassic, Northern Alps, Austria). *Facies,* 38: 207-228, Erlangen.

Finetti I.R. (2005) - Understanding the Ionides. In: Finetti, I.R. (Ed.) - CROP - Deep Seismic Exploration of the Mediterranean Region. Atlases in Geoscience, 1: 197-208, Elsevier, Amsterdam.

Fischer A.G. (1964) - The Lofer cyclothems of the Alpine Triassic. *Kansas Geol. Surv. Bull.,* 169: 107-149, Lawrence.

Flügel E. (2002) - Triassic reef patterns. In: Kiessling W. et al. (Eds) - Phanerozoic reef patterns: *SEPM (Society for*

Sedimentary Geology), Spec. Publ., 72: pp. 391-463, Tulsa.

Foos A.M. (1991) - Aluminous lateritic soils, Eleuthera, Bahamas: a modern analog to carbonate paleosols. *J. Sediment. Petrol.,* 61: 340-348, Tulsa.

Galli M.T., Jadoul F., Bernasconi S. & Weissert H. (2005) - Anomalies in global carbon cycling and extinction at the Triassic/Jurassic boundary: evidence from a marine C-isotope record. *Palaeogeogr. Palaeoclimat. Palaeoecol.*, 216: 203-214, Amsterdam.

Galli M.T., Jadoul F., Bernasconi S. Cirilli S. & Weissert H. (2007) - Stratigraphy and palaeoenvironmental analysis of the Triassic-Jurassic transition in the western Southern Alps (Northern Italy). *Palaeogeogr. Palaeoclimat. Palaeoecol.*, 244: 52-70, Amsterdam.

Gazdzicki A. (1983) - Foraminifers and biostratigraphy of Upper Triassic and Lower Jurassic of the Slovakian and Polish Carpathians. *Acta Palaeont. Pol.*, 44: 109-169, Warszawa.

Ginsburg R.N. & Hardie L.A. (1975) - Tidal and storm deposits, northwestern Andros Island, Bahamas. In: Ginsburg RN (Ed) - Tidal deposits: a casebook of recent examples and fossil counterparts, 8: 201-208, Springer, Berlin, Heidelberg, New York.

Goldhammer R.K., Dunn P.A. & Hardie L.A. (1990) - Depositional cycles, composite sea-level changes, cycle stacking patterns, and the hierarchy of stratigraphic forcing: examples from Alpine Triassic platform carbonates. *Geol. Soc. Am. Bull.,* 102: 535-562, Tulsa.

Haas J. (1994) - Lofer cycles of the Upper Triassic Dachstein platform in the Transdanubian Mid-Mountains (Hungary). *Int. Assoc. Sedimentol.*, Spec. Publ., 19: 303-322, Oxford.

Haas J. (2004) - Characteristics of peridídal facies and evidences for subaerial exposures in Dachstein-type cyclic platform carbonates in the Transdanubian Range, Hungary. *Facies,* 50: 263- 286, Erlangen.

Haas J. & Skourtsis-Coroneou V. (1995) - The Upper Triassic platform sequences in the Transdanubian Range and the Pelagonian Zone SL: a correlation. *Geol. Soc. Greece,* Spec. Publ., 4: 195-200, Athens.

Haas J. & Tardy-Filácz E. (2004) - Facies changes in the Triassic-Jurassic boundary interval in an intraplatform basin succession at Csovár (Transdanubian Range, Hungary). *Sediment. Geol.*, 168: 19-48, Amsterdam.

Hallam A. (1981) - The end-Triassic bivalve extinction event. *Palaeogeogr. Palaeoclimat. Palaeoecol.*, 35: 1-44, Amsterdam.

Hallam A. (1990) - Correlation of the Triassic-Jurassic boundary in England and Austria. *J. Geol. Soc.*, 147: 421-424, London.

Hallam A. (1991) - Discussion of the Triassic-Jurassic boundary of England and Austria. *J. Geol. Soc.*, 148: 420-422, London.

Hallam A. (1995) - Oxygen-restricted facies of the basal Jurassic of north west Europe. *Hist. Biol.*, 10: 247-257, London.

Hallam A. (1997) - Estimates of the amount and rate of sea-level change across the Rhaetian-Hettangian and Pliensbachian-Toarcian boundaries (latest Triassic to early Jurassic). *J. Geol. Soc.*, 164: 1093-1108, London.

Hallam A. & Goodfellow W.D. (1990) - Facies and geochemical evidence bearing on the end-Triassic disappearance of the Alpine reef ecosystem. *Hist. Biol.*, 4: 131-138, London.

Hallam A. & Wignall P.B. (1999) - Mass extinctions and sea-level changes. *Earth-Sci. Rev.*, 48: 217-250, Amsterdam.

Hesselbo S.P., Robinson S.A. & Surlyk F. (2004) - Sea-level change and facies development across potential Triassic - Jurassic boundary horizons, SW Britian. *J. Geol. Soc.*, 161: 365-379, London.

Hesselbo S.P. McRoberts C.A. & Pálfy J. (2007) - Triassic-Jurassic Boundary events: problems, progress, possibilities. *Palaeogeogr. Palaeoclimat. Palaeoecol.,* 244(1-4): 1-424, Amsterdam.

Hardie L.A. & Shinn E.A. (1986) - Carbonate depositional environments, modern and ancient, Tidal flats. *Colorado School Mines Q.*, 81: 1-74, Golden.

Hottinger L. (1983) - Processes determining the distribution of larger foraminifera in space and time. In: Meulenkamp J.E. (Ed.) - Reconstruction of marine paleoenvironments. *Micropal. Bull.*, 30: 239-253, Utrecht.

Hottinger L. (1967) - Foraminifères imperforés du Mésozoïque marocain. *Notes et Mém. Serv. Géol. Maroc*, 209, 168 pp., Rabat.

Jadoul F., Berra F. & Frisia S. (1992) - Stratigraphic and paleontologic evolution of a carbonate platform in an extensional tectonic regime: example of the Dolomia Principale in Lombardy (Italy). *Riv. It. Paleont. Strat.*, 91: 479-511, Milano.

Katsikatsos G. (1979) - La structure tectonique d' Attique et de l'île d' Eubée. VI Coll. on the Geol. of the Aegean Region, Athens 1977, Proceedings, Vol. 1: 211-220, IGME, Athens.

Krystyn L., Bouquerel H., Kuerschner W., Richoz S. & Gallet Y. (2007) - Proposal for a candidate GSSP for the base of the Rhaetian Stage. In: Lucas S.G. and Spielmann J.A. (Eds) - 2007, The Global Triassic. *New Mexico Museum of Natural History and Science Bulletin,* 41: 189-199, Albuquerque.

Masetti D., Claps M., Giacometti A., Lodi P. & Pignatti P. (1998) - I Calcari Grigi della Piattaforma di Trento. *Att. Tic. Sc. Terra*, 40: 139-183, Pavia.

Masetti D., Fantoni D., Romano R., Sartorio D., Trevisani E. & Venturini S. (2006) - Stratigraphy, architecture and paleogeographic evolution of the exentional basin in the Eastern Southern Alps. *Volumina Jurassica*, IV: 97-98, Warszawa.

Masetti D., Neri C., Stefani M. & Zanella R. (1985) - Cicli e tempestiti nel 'Retico' delle Dolomiti di Brenta. *Mem. Soc. Geol. Ital.*, 30: 267-283, Roma.

McRoberts C.A., Furrer H. & Jones D.S. (1997) - Palaeoenvironmental interpretation of a Triassic-Jurassic boundary section from western Austria based on palaeoecological and geochemical data. *Palaeogeogr. Palaeoclim. Palaeoecol.*, 136: 79-95, Amsterdam.

Michalík J., Lintnerová O., Gazdzicki A. & Soták J. (2007) - Record of environmental changes in the Triassic-Jur-

assic boundary interval in the Zliechov Basin, Western Carpathians. *Palaeogeogr. Palaeoclim. Palaeoecol.*, 244: 71-88, Amsterdam.

Moix P., Kozur H.W., Stampfli G.M. & Mostler H. (2007) - New Paleontological, biostratigraphical and Paleogeographic results from the Triassic of the Mersin Mélange, SE Turkey. In: Lucas S.G. & Spielmann J.A. (Eds) 2007 - The Global Triassic. *New Mexico Museum of Natural History and Science Bulletin,* 41: 282-311, Albuquerque.

Pálfy J., Demény A., Haas J., Carter E.S., Görög Á., Halász D., Oravecz-Scheffer A., Hetényi M., Márton E., Orchard M.J., Ozsvárt P., Vető I. & Zajzon N. (2007) - Triassic-Jurassic boundary events inferred from integrated stratigraphy of the Csővár section, Hungary. *Palaeogeogr. Palaeoclim. Palaecol.*, 244: 11-33, Amsterdam.

Parginos D., Mavrides A., Bornovas I., Mettos A., Katsikatsos G., Koukis G., Christodoulou G., Tsaila-Monopolis St., Skourtsis-Koroneou B., Ioakim Ch., Dimou-Honianaki E. & Kanaki-Mavridou F. (2007) - Geol. map of Greece 1:50 000, sheet "Halkida", IGME, Athens.

Partsch J. (1887) - Die Insel Korfu. - Petermanns Mitteilungen, Ergzungsheft, 19/88: 1-97, Gotha.

Petti F.M. (2007) - Formazione Inici. Carta Geologica d'Italia 1:50.000 - *Quaderni del servizio Geologico d'Italia- Catalogo delle Formazioni* - Serie III, 7(VI): 259-270, Roma.

Pomoni-Papaioannou F., Trifonova E., Tsaila-Monopolis ST. & Katsavrias N. (1986) - Lofer type cyclothems in a Late Triassic dolomitic sequence on the eastern part of the Olympus. IGME *Geol. Geophys. Res.* Spec. Issue: 403-417, Athens.

Renz C. & Reichel M. (1948) - Neue Foraminiferen funde im boeotischen Seegebiet (Mittelgriechenland). *Ecl. geol. Helv.,* 41: 379-389, Basel.

Satterley A.K. (1996) - The interpretation of cyclic succession of the Middle and Upper Triassic of the Northern and Southern Alps. *Earth Sci. Rev.,* 40: 181-207, Amsterdam.

Satterley A.K. & Brandner R. (1995) - The genesis of Lofer cycles of the Dachstein Limestone, Northern Calcareous Alps, Austria. *Geol. Rundsch.*, 84: 87-292, Stuttgart.

Schäfer P. & Senowbari-Daryan B. (1982) - The Upper Triassic Pantokrator Limestone of Hydra (Greece): An example of a prograding reef complex. *Facies*, 6: 147-163, Erlangen.

Schwarzacher W. & Haas J. (1986) - Comparative statistical analysis of some Hungarian and Austrian Upper Triassic peritidal carbonate sequences. *Acta Geol. Hung.,* 29: 175-196, Budapest.

Sepkoski J.J. (1996) - Patterns of Phanerozoic extinction: a perspective from global data bases. In: Walliser, O.H. (Ed.) - Global Evens and Event Stratigraphy in the Phanerozoic. Springer: 21-35, Berlin.

Septfontaine M. (1984) - Biozonation (a l'aide des foraminifères imperfores) de la plate-forme interne carbonatée Liasique du Haut Atlas. *Rev. Micropaléont.*, 27: 209-229, Paris.

Septfontaine M. (1986) - Mileux de depôts et foraminifères (Lituolides) de la plate-forme carbonatée du Lias Moyen au Maroc. *Rev. Micropaléont.*, 28: 265-289, Paris.

Schlager W. (2005) - Carbonate Sedimentology and Sequence Stratigraphy. *SEPM Concepts in Sedimentology and Paleontology*, 8, 200 pp., Tulsa.

Shinn E.A. (1983) - Tidal flat environment. In: Sholle P.A., Bebout D.G. & Moore C.H. (Eds) - *AAPG Mem.*, 33: 173-210, Tulsa.

Stampfli G.M. & Borel G.D. (2002) - A plate tectonic model for the Paleozoic and Mesozoic constrained by dynamic plate boundaries and restored synthetic oceanic isochrons. *Earth Planet. Sci. Lett.*, 196: 17-33, Amsterdam.

Tanner L.H., Lucas S.G. & Chapman M.G. (2004) - Assessing the record and causes of Late Triassic extinctions. *Earth-Sci. Rev.,* 65: 103-139, Amsterdam.

Tataris A., Kounis G., Maragoudakis N., Christodoulou G., Bizon G. & Tsaila-Monopolis St. (1970) - Geol. map of Greece 1:50 000, Sheet "Thivai", I.G.S.R., Athens.

Wilmsen M. & Neuweiler F. (2008) - Biosedimentology of the Early Jurassic post-extinction carbonate depositional system, central High Atlas rift basin, Morocco. *Sedimentology,* 55: 773-807, Oxford.

Wright V.P. (1994) - Paleosols in shallow marine carbonate sequences. *Earth - Sci. Rev.* 35: 367-395, Amsterdam.